Jari Torniainen

Modeling early neural responses according to low-level parameters of visual stimuli

School of Electrical Engineering

Thesis submitted for examination for the degree of Master of Science in Technology.

Espoo 8.12.2014

Thesis supervisor:

Prof. Raimo Sepponen

Thesis advisor:

D.Ph. (Psych.) Jaana Simola

Aalto University
School of Electrical
Engineering

AALTO UNIVERSITY
SCHOOL OF ELECTRICAL ENGINEERING

ABSTRACT OF THE
MASTER'S THESIS

Author: Jari Torniainen

Title: Modeling early neural responses according to low-level parameters of visual stimuli

Date: 8.12.2014 Language: English Number of pages: 7+59

Department of Electrical Engineering and Automation

Professorship: Electrical Engineering and Automation Code: S-55

Supervisor: Prof. Raimo Sepponen

Advisor: D.Ph. (Psych.) Jaana Simola

Introduction
Experiment consisting of a visual search was conducted in order to investigate the effect of top-down and bottom-up processing with natural stimuli. Gray-scale photographs of nature scenes were used as stimuli. Stimuli had two conditions: natural and scrambled. Natural images were unaltered photographs and in scrambled images the global information was reduced.
Aim
Aim of the experiment was to form statistical models explaining the effect the amplitude of early visual potentials as functions of visual input, oculomotor variables and top-down factors.
Methods
Magnetoencephalography (MEG), electroencephalography (EEG) and eye tracking were recorded simultaneously during the experiment. In the scope of this thesis only EEG and eye tracking were analysed. Statistical models were generated using a method called linear mixed (effect) modeling.
Results
Data analysis produced two models describing the early visual potential as parameters of visual input and oculomotor variables. The effect of top-down processing was investigated as an additional statistical test.
Conclusion
Out of the two generated models the visual input model was deemed more accurate due to spatial focality and amplitude latency. Results of the study indicate that early visual responses in EEG correlate strongly with low-level visual inputs and to a lesser degree with oculomotor variables. No evidence of correlation between response amplitude and top-down factors were observed.

Keywords: EEG, MEG, Eye-tracking
Visual attention

AALTO-YLIOPISTO
SÄHKÖTEKNIIKAN KORKEAKOULU

DIPLOMITYÖN
TIIVISTELMÄ

Tekijä: Jari Torniainen

Työn nimi: Varhaisten visuaalisten EEG vasteiden mallintaminen kuva-ärsykkeen ominaisuuksien mukaan

Päivämäärä: 8.12.2014 Kieli: Englanti Sivumäärä: 7+59

Sähkötekniikan ja automaation laitos

Professuuri: Sähkötekniikka ja automaatio Koodi: S-55

Valvoja: Prof. Raimo Sepponen

Ohjaaja: FT Jaana Simola

Johdanto
Visuaalista tarkkaavaisuutta tutkittiin koeasetelmassa, jossa koehenkilöt etsivät heille esitettyjä kuvan osia suuremmista luontovalokuvista. Kuvia oli kahta tyyppiä: muokkaamattomia, sekä kuvia joista globaali informaatio oli hävitetty.
Tavoite
Kokeen tavoitteena oli kehittää visuaalisia hermostovasteita kuvaava tilastollinen malli. Mallin avulla oli tarkoitus tutkia kuinka matalan ja korkean tason tarkkaavaisuusprosessit vaikuttavat mitattuun vasteeseen.
Menetelmät
Kokeen aikana koehenkilöiltä mitattiin aivosähkökäyrää (EEG), aivomagneettikäyrää (MEG) sekä silmänliikettä. Kerätty data analysoitiin mallintamalla katseeseen synkronisoituja EEG-vasteita tilastollisesti. Kokeessa kerättyä MEG dataa ei analysoitu tämän työn puitteissa. Mallintamiseen käytettiin lineaarisia sekamalleja, jotka muodostettiin ärsykekuvien, silmänliikkeiden ja tarkkaavaisuusprosessien avulla.
Tulokset
Mallintaminen tuotti kaksi erilaista mallia, jotka selittivät syntyneen vasteen visuaali-informaation ja silmänliikkeiden perusteella. Korkean tason tarkkaavaisuuden vaikutusta tutkittiin molemmissa malleissa ylimääräisellä tilastollisella testillä.
Johtopäätökset
Kahdesta tuotetusta mallista visuaalimalli vaikutti todenmukaisemmalta. Silmänliikemallin tulokset olivat puolestaan epävarmempia sijaintinsa ja esiintymislatenssinsa takia. Kummankaan mallin tapauksessa ei havaittu todisteita korkean tason tarkkaavaisuuden vaikutuksesta vasteisiin.

Avainsanat: EEG, MEG, Silmänliikemittaus
Visuaalinen tarkkaavaisuus

Preface

I'd like to thank my family, friends and my advisor for helping me complete this thesis.

Otaniemi, 8.12.2014

Jari E. Torniainen

Contents

Abstract ii

Abstract (in Finnish) iii

Preface iv

Contents v

Symbols and abbreviations vii

1 Introduction 1

2 Background 3
2.1 Vision and visual attention . . . 3
2.2 Experimental setups in psychophysical experiments . . . 6
2.3 Recording methods and apparatus . . . 8
2.3.1 Eye tracking methodology . . . 8
2.3.2 EEG and MEG . . . 11
2.3.3 Co-registration . . . 12
2.4 Event related potentials . . . 14
2.4.1 Event related potential technique methodology . . . 14
2.4.2 Visually evoked potentials . . . 15
2.5 Linear Mixed Effect Model . . . 17

3 Materials and methods 19
3.1 Experimental design and implementation . . . 19
3.2 Acquisition . . . 20
3.2.1 Apparatus . . . 20
3.2.2 Quantifying the spatial accuracy of the eye tracker . . . 23
3.2.3 Temporal synchronization of the acquisition devices . . . 24
3.3 Procedure . . . 26
3.4 Preprocessing . . . 28
3.5 Statistical analysis of the collected data . . . 29
3.5.1 Outline of the analysis . . . 29
3.5.2 Selection of independent fixed-effects . . . 32
3.5.3 Selection of mixed-effects . . . 33
3.5.4 Formulation of the statistical model . . . 35
3.5.5 Reduction of the model . . . 37
3.5.6 Statistical significance testing . . . 39

4 Results 40

5 Summary and discussion 45
5.1 Evaluation of the experimental design and implementation . . . 45
5.2 Evaluation of results . . . 45

5.2.1 Visual model 46
5.2.2 Oculomotor model 46
5.2.3 Top-down vs. bottom-up processing 47
5.3 Global normalization 47

6 Future research **49**

References **50**

A Visual model coefficients **57**

B Oculomotor model coefficients **58**

Symbols and abbreviations

Symbols

Operators

Abbreviations

AIC	Akaike information criterion
BCI	Brain-computer interface
BIC	Bayesian information criterion
BOLD	Blood oxygen level dependent (response)
EEG	Electroencephalography
EOG	Electrooculography
ERP	Event-related potential
fMRI	Functional magnetic resonance imaging
HCI	Human-computer interaction
HPI	Head position indicator
IR	Infrared
KLD	Kullback-Leibler distance
LMM	Linear mixed (effect) model
LRT	Likelihood ratio
MEG	Magnetoencephalography
ML	Maximum likelihood
MRI	Magnetic resonance imaging
PCA	Principal component analysis
REML	Restricted maximum likelihood
SOA	Stimulus onset asynchrony
SP	(Saccadic) Spike potential
SSIM	Structural similarity index
SQUID	Superconducting quantum interference device
TEVSOC	Towards ecologically valid study of cognition
TTL	Transistor to transistor logic
VEP	Visually evoked potential

1 Introduction

Towards Ecologically Valid Study of Cognition (TEVSOC) was a research project conducted at Cognitive Science Division of the University of Helsinki between 2011 - 2014. The project was funded by the Academy of Finland and this thesis was conducted as a part of TEVSOC project. The aim was to develop and improve the methodology for naturalistic visual attention studies. The experiment was partly cognitive neuroscience and partly vision research. Data acquisition of the experiment was conducted in the BioMag Laboratory at Helsinki University Central Hospital with the approval from the board of ethics and in accordance to declaration of Helsinki [1]. This thesis outlines the entire process from designing the experiment to the analysis of the results while maintaining a technical viewpoint. The thesis specifically attempts to address all the technical challenges involved in recording and analysing multiple-source neurological data in a psychophysical experiment.

The experiment aimed to investigate the effect of local and global visual information to early neural responses of visual processing. The stimuli consisted of 70 grayscale nature photographs selected from an existing picture database. In each trial of the experiment the subject was first shown a small portion of an image followed by a larger image. The subject was then asked if the first fragment could be found in the following larger image. A total of 28 volunteers (mostly students) participated in the experiment. During the experiment both electroencephalography (EEG) and magnetoencephalography (MEG) were recorded. A remote eye tracker was also used to capture participants' eye movements during the presentation of the stimuli. Combination of the two recording methodologies gives information about where and when the subjects were looking at and what the neural activity was during the visual search task. This setup is coined co-registration [2] and is an emerging research tool in psychological research. By utilizing co-registration, the experiment was implemented as a free-viewing paradigm, that is, the subjects were free to examine the presented stimulus without any constraints to eye movements. Free-viewing is a relatively novel experimental paradigm made possible by the recent increase in the availability of commercial eye trackers. The triple registration of eye tracking, EEG and MEG is also a relatively new recording technique and during the writing of this thesis no earlier research had recorded these three datasets simultaneously. Due to the complexity of synchronizing three different recording apparatus the implementation of the experiment proposed some interesting technical challenges. A more in-depth description of the stimuli, experimental setup and recording apparatus can be found in section 3.

The experiment had two main objectives. The first aim was to study and improve the ecological validity of psychophysical experiments in the field of visual attention research. The term *ecologically valid* in this context implies to experimental setups where the conditions of the experiment are as close as possible to real life. This is a contrast to more traditional setups where the experimental conditions are tightly controlled in order to simplify the data analysis. One example of these constraints

is the aforementioned restriction of eye movements. Eye movements are normally restricted in EEG/MEG experiments because they generate artifacts in the recorded signal due to the electric properties of the human eye. The artifact signal is of a much higher amplitude than the underlying neural signal source and thus masks the responses that these experiments are trying to study. With the advance of recording technology and techniques, however, it is now possible to relax some of these constraints and compensate for the artifacts using the data gathered with the eye tracker. This change in paradigm, in turn, brings up some challenges regarding the synchronization of multiple recording devices that must be addressed. The second objective was to form a statistical model to explain the contributions of different factors on the recorded neural responses. These factors included variables calculated from the visual input (such as the relative luminance and contrast of the observed region of the stimuli) as well as oculomotor variables. These low-level covariates of visual attention are commonly known as bottom-up processing. The analysis focused on the so called early visual responses which occur approximately 50-100 ms after the intake of visual information. Effect of higher level processes of visual attention (also known as top-down processing) on the early visual responses was also investigated. These higher level processes include such cognitive functions as memory and intention. The aim of the data analysis was to produce a comprehensive model of the early visual potentials by combining both the top-down and bottom-up processing as well as the oculomotor processes.

The first part of this thesis covers the theoretical background of visual attention, experimental designs, recording methods and statistical models. Second part focuses on the practical implementation of the experiment, recording procedure and data analysis. Finally, the third part consists of reporting the results of the analyses performed and estimating the accuracy of these results. The experiment provided enough data for multiple different analyses and hypothesis tests. The possible courses for future research with the collected data are also outlined at the end of this thesis.

2 Background

2.1 Vision and visual attention

Visual attention is a process which selects and limits the intake of information from our surroundings. Vision is arguably the most important sensory input for humans and is thus a widely researched topic. Research on visual attention aims to integrate the neural pathways of vision and neural processing of visual information to behavioral results observed when images are being studied. Most theories agree that visual attention is guided by two competing mechanisms: the top-down and the bottom-up [3]. In bottom-up processing attention is attracted to salient and prominent visual features of the perceived stimulus [4]. These salient features present a pop-up effect which automatically capture and attract attention. Top-down model on the other hand describes attention as a combination of higher level cognitive functions [5]. These functions include such processes as memory, intention and emotions. In the light of earlier research it appears that visual attention is guided by an interplay of both processes [6]. This section very briefly outlines the physiological basis of visual attention by covering functions of the eyes and the human visual system.

Human vision is a complex system of sensory organs and neural pathways that transform incoming light into a representation of the surrounding space and objects within the field of view. The first step in this processing chain are the eyes which acquire the visual information. Human eye consists of a ball-shaped sensory organ filled with viscous fluid and enveloped inside three layers of membrane. The frontal surface of the eyeball contains a transparent outer layer known as the cornea and a ligament-suspended lens. Light reflected from objects travel through this lens to the rear surface of the eye where it is encoded and passed forward through the visual system. The lens is surrounded by a ring-like group of ciliary muscles which control the shape of the lens. Changes in lens geometry enables the viewing of objects at varying viewing distances. The rear inner surface of the eye contains an area known as the retina which consists of a dense cluster of light sensitive sensor cells knowns as photoreceptors. These photoreceptors electrochemically encode the incoming light into electric signals and pass them on to the brain through the optic nerve. The optic nerve travels through the visual pathway eventually reaching the visual cortex of the occipital lobe where the actual neural processing of the visual information starts. The retina houses two types of photoreceptors: rod-cells for dim light and cone-cells for perception of color and fine detail. Photoreceptors are not distributed equally over the retina and the center of the retina has a considerably higher density of cone-cells. Due to the nonuniform distribution only a small portion of the total field of view can be observed with high visual acuity at any given time. The region of high visual acuity is known as the *fovea centralis* (abbreviated to fovea in most literature) which is a dense cluster of cone-type photoreceptors located in the part of the retina known as macula. Visual acuity decreases rapidly as distance from the center of the fovea increases and the high acuity region is roughly 2 degrees

of the visual field. In order to accurately perceive objects within the field of view the eyes must constantly move. Detecting objects outside the fovea is also possible but with dramatically impaired accuracy. The surrounding field between 3 to 5 degrees of the visual field around fovea is known as the parafovea. The area around the parafovea is known as the peripheral visual field which reaches out to about 10 degrees of the total visual field. Structure of the eye can be seen in figure 1. Connected to each eyeball are six muscles which enable the various rotational movements. Eyes are capable of conducting different kinds of movement as a part of the complex physiological negative-feedback system of human vision. In the case of a static visual stimuli (such as a picture displayed on a computer monitor) the two main movement types that occur are saccades and fixations. Saccades are rapid transitions of the eye which shift the location of the fovea [7]. The transitions are preprogrammed "leaps" during which the eye is effectively blind due to a mechanism called saccadic suppression [8]. The velocity profile of a saccade roughly follows a bell curve. Fixations on the other hand are time periods when the eye is stationary and relatively stable. During fixations the information is being acquired by the retina, encoded into electrical signal and passed forward through the optic nerve. Duration of the fixations change depending on the task being performed. For example, the fixation duration in a visual search task is usually shorter than when reading text [9]. Eye does not, however, remain absolutely stable during a fixation. In reality fixations contain a subset of "micro movements" which facilitate the intake of visual information. These micro movements are often in the order of 5 to 100 arc-minutes of the visual field. Purpose of the micro movements is not entirely clear but is thought to acts as a countermeasure for drifts and the image fading from the fovea [10]. In the case of a moving target the eyes perform a motion known as smooth pursuit [11]. Smooth pursuit allows tracking of moving objects and normally can not be performed without a moving stimulus. Because the performed experiment involved static picture stimuli, only fixations and saccades will be discussed in the further chapters. [12]

In the human visual system the retina can be considered to be the input layer for incoming visual information. In addition to photoreceptors the retina also houses horizontal, bipolar, amacrine and ganglion cells related to the processing of incoming light. The structure of the retina is layered, with photoreceptors at the bottom of the retina and other cell groups on top. A diagram of this structure is displayed in figure 2. The role of amarcine, bipolar and horizontal cells is to further compress the electrical signals generated by the photoreceptors before it reaches the ganglion cells. The information is subsequently passed forward from the retina by the axons of the ganglion cells on top of the retinal cell-layer. Axons exit the optic disc in a bundle of fiber-like axons known as the optic nerve. The optic nerve splits at the optic chiasm where about 60% of the fibers of the optic nerve cross the chiasm and 40% stays on the same side. After the optic chiasm the bundles on each side contain information from both eyes and are known as optic tracts. The bundles of the optic tract diverge to multiple different regions of the brain. Part of the fibers travel to regions that control the motoric functions of the eyes (superior colliculus) and part to the region

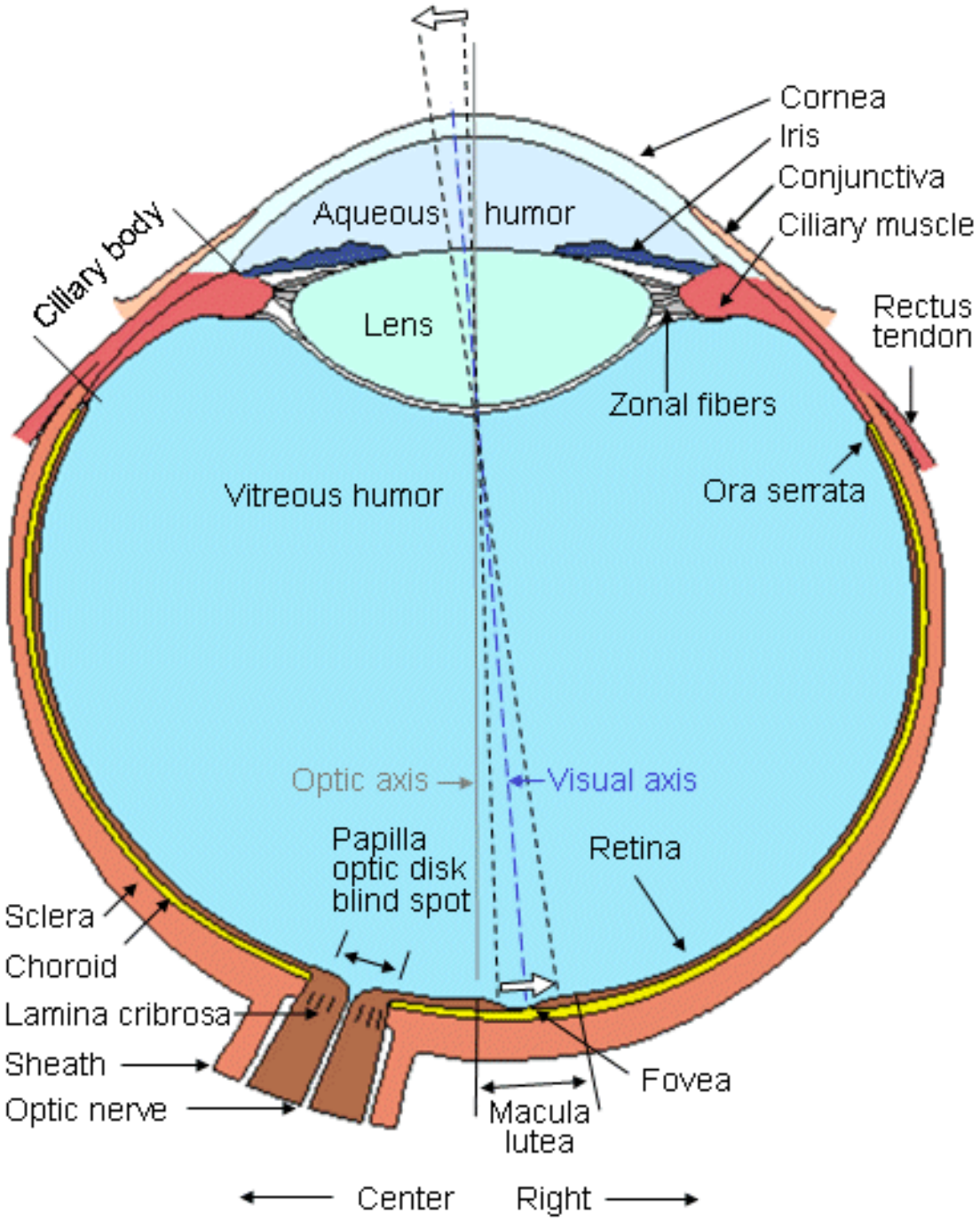

Figure 1: Structure of the human eye [13].

responsible for the pupillary reflex (pretectum) and to other components of the feedback system. Eventually the optic tract reaches the cortex of the occipital lobe which is also known as the visual cortex. Visual cortex is where the decoding and processing of the visual information starts. Eventually the information will advance towards frontal regions of the brain via temporal (also known as ventral-pathway) and parietal (also known as dorsal-pathway) pathways [14] but information is also

fed back to the sensory areas [15]. In the study of visual potentials the responses recorded from the visual cortex are of the key interest. Technically it is possible to record the responses of the visual stimulation from deeper brain structures, such as pretectum or superior colliculus, using a method with sufficient penetration and sensitivity to deep sources (i.e. MEG or fMRI) [16]. Although these responses could in some sense be called visual potentials, in the context of this study and most of the supporting literature, the term visual potential is reserved for the neural responses recorded from the visual cortex of the occipital lobe. It is these visual potentials (more specifically the very early ones) that were also the key interest in the experiment.

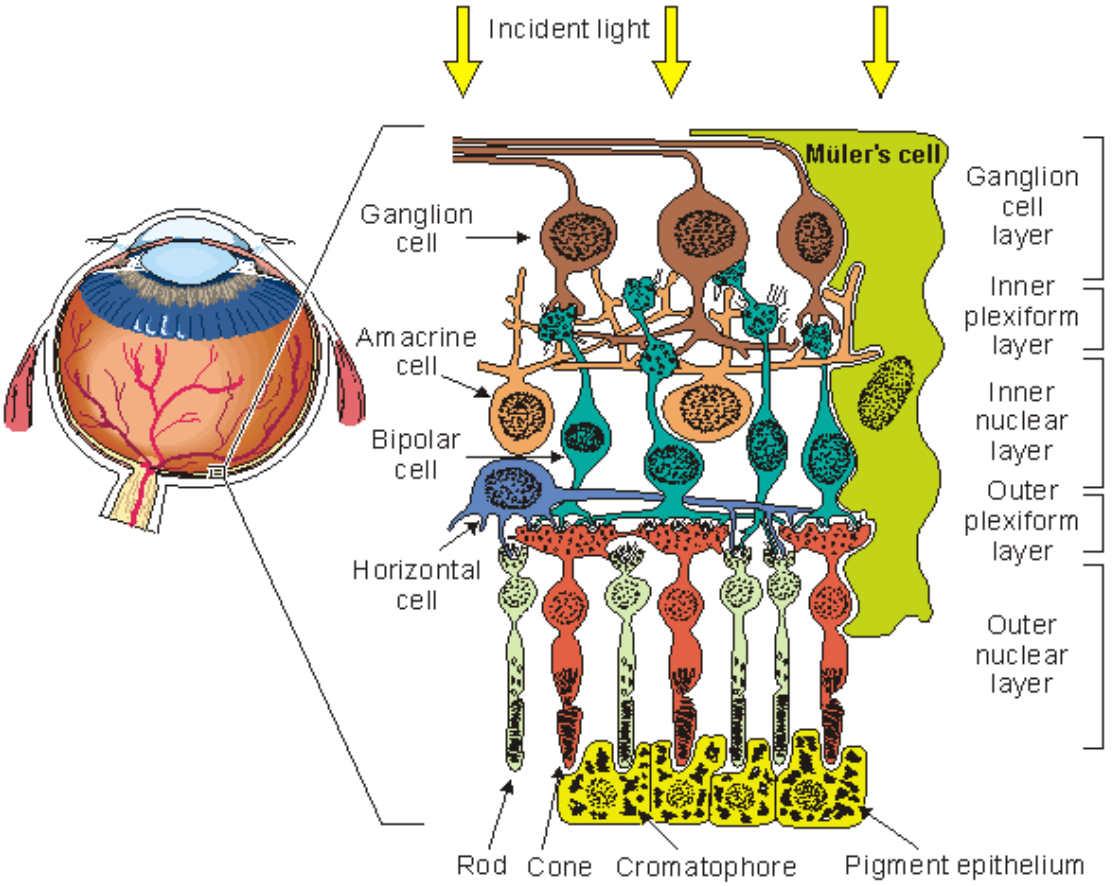

Figure 2: Cell layers of the retina [17].

2.2 Experimental setups in psychophysical experiments

In experimental psychology the design and careful control of confounding factors is an integral part of any research project. This section is intended to give a brief overview of what kind of preparatory work the experiment required. It will cover such topics as factor control, within/between subject paradigms, stimulus onset

asynchrony (SOA) and blocking. These aspects are important for stimulus preparation, programming of the experiment and setting up the triggering signals.

In the context of experimental design all parameters of the experiment are called factors. Aim of the design is to produce a paradigm where the factors of interest (i.e. the variables whose effect on the measured quantity is being investigated) are controlled with respect to all other factors As such all non-crucial factors should be processed into as uniform as possible. In the case of photographs this means normalizing the properties of all stimuli according to some condition. Possible methods include matching luminance histograms [18] or normalizing the spectral content of different frequency bands [19]. In designing the experiment important step is to decide which factors are controlled and to what degree. Presentation order of the stimuli is also an important design decision. In order to counter systematic effects randomization of the order in which subjects are exposed to stimuli of different conditions should be used.

Another question regarding the setup is whether the experiment follows a *between-subjects* or *within-subjects* paradigm. In between-subjects design a different population is used for different stimulus group (essentially dividing the pool of participants based on predefined conditions). In a within-subject paradigm all subjects are exposed to the same stimuli. Both approaches have their advantages and disadvantages [20]. The benefit of within-subject paradigm is that the subject pool is considerably larger due to all subjects being in one group. Additionally, in between-subject paradigms it is possible that the subjects have been divided in a way where individual differences become a factor in the results. The major downside of within-subject is the interconnectivity of tasks and stimuli within the experiment, also known as the *carryover effect*. In carryover effect some of the conditions in the experiment influence the performance and/or response in other conditions [21]. This of course is not a problem in between-subject paradigm as the experimental conditions are separated into groups. Furthermore, fatigue can be an issue in a prolonged within-subject paradigms as it can affect both behavioral results and neural responses.

In experiments where neural responses are recorded anticipatory effects become a real problem. When nearly identical stimulus is repeated at a constant rate the subject becomes habituated to it and the related responses are often dampened. To counter this the interval between stimuli is often randomized. This process is known as stimulus onset asynchrony or SOA for short [22]. Randomization of the onset will also prevent the phase-locking of responses. SOA is more important in experiments where the stimulus is presented in a rapid succession but it is good practice to control it in all experiments.

Blocking in experimental design means dividing the experiment into segments. Blocking can be done according to some variable or alternatively just to reduce the fatigue factor of the experiment. There are multiple ways of performing blocking with regards to the order in which blocks are ran and the randomization of the content inside each block [23].

Finally the actual implementation of the experiment is the last step but also a very important one. In experiments where a physiological variable is being measured the temporal accuracy is of critical importance. The timing of stimulus presentation must be controlled to the order of milliseconds. For this purpose there exists a wide range of stimulus presentation softwares. Most of these provide the tools to program the experimental design. These programs range from visual modeling languages (ExperimentBuilder, E-Prime) to more traditional Java-style programming (Presentation). Both of these programs are commercial but Python-based open-source solutions like PsychoPy [24] and MATLAB based psychotoolbox exist as well. The most important thing for the stimulus presentation environment is the temporal accuracy, i.e. the time delay between the command to display the stimulus and actually drawing it on the monitor or screen. The second important feature of stimulus presentation software is their connectivity to recording devices. In addition to accurately displaying stimulus the software must be able to signal the recording device when subject was exposed to the stimulus. This process is known as triggering and it is used to add markers in the data streams for later analysis. Different softwares support different protocols for triggering but the most common interfaces are the parallel port and the Ethernet protocol.

2.3 Recording methods and apparatus

2.3.1 Eye tracking methodology

Eye tracking technology has been around for closer to 50 years now and the first gaze tracking experiments were performed already in the 1930s. The term *eye tracking* usually means the tracking of the location and orientation of the human eye and then calculating a projection indicating the location of the gaze. With this method it is possible to determine where and when the test subject was looking at. In typical setups the subject is looking at a computer monitor with the eye tracker positioned in front of them although other methods for presenting the stimulus could also be used. A wide range of different eye tracking devices exist today ranging from laboratory measurement devices to portable ones. Applications of eye tracking include usability research, human-computer interfaces (HCI) [25], marketing research [26] as well as basic psychological research [27]. Eye-tracking is a valuable research tool in visual attention as properties of the eye movements change during the analysis of visual scenes [28].

To date various different methods and devices for tracking eye movements exist [29]. Throughout the development of eye trackers the method for capturing the eye orientation has changed drastically. Earliest devices relied on the electric fields generated by eye movements using a technique more commonly known as electrooculography (EOG). These fields are recordable with standard EEG setups and most EEG montages included additional bipolar EOG-electrodes for more accurate eye-movement registration. Using two sets of bipolar EOG electrodes placed around the eyes it

is possible to detect both horizontal and vertical shifts in the direction of the gaze along with eye blinks. As stated earlier, in traditional sense, the EOG signal is considered to be an artifact that masks the underlying EEG activity. EOG has, however, been utilized in various BCI experiments for acting as a rough estimate of the direction of the gaze [30]. Advantages of EOG-based eye tracking include high temporal resolution (same as EEG) and relatively low instrumentation cost. Downside to this method is poor spatial accuracy [32]. Another method of tracking eye movements is to use contact lenses. With this method the basic principle is to use a contact lens attached on top of the eye to relay information about the orientation of the eye. The method of receiving the information of the orientation varies between methods. One example is the relatively old method of conducting the measurement inside an alternating magnetic field with coils integrated into the contact lenses [31]. Changes in the orientation of the lens can then be measured from induction current and converted into gaze coordinates. While this method can produce spatially accurate results the setup is technically challenging. Furthermore the setup can be uncomfortable for the subject being measured. Some earlier research also indicates that the eye movements differ from normal when a load (such as a contact lens) has been attached to it. The artificial change in eye movement parameters might be undesirable if the object of the experiment is to study visual attention. Today optical video-based methods are the most common way of performing eye tracking. Earliest video-based trackers simply recorded eye movements and the calculation of the gaze point was done manually by superimposing the gaze coordinates on top of the viewed stimulus. With more advanced computer vision applications and increase in computation speed it later became possible to automate the entire process. Today nearly all of the commercially available eye trackers are based on infrared (IR) video cameras with an external IR light source and automated software for processing the captured images.

Video-based eye trackers have revolutionized the field of eye movement research [32]. These devices record image of the eye (or eyes) and calculate the gaze location for each recorded frame. Video-based eye trackers often use infrared (IR) cameras and external IR light sources for tracking but devices that operate with normal cameras also exist [33]. The benefit of using IR is to assert that the only source of reflections on the eye is caused by the measuring device. For successful tracking the measurement site should of course not have any other IR light sources present which makes outdoor recordings difficult. The method is based on focusing the camera on the eye and extracting the location of the pupil and the first *Purkinje reflection*. Purkinje reflection is the IR light reflected back from the cornea of the eye. Extracting the center of the pupil and the location of the corneal reflection in prespecified calibration points makes it possible to interpolate the gaze point in all other areas inside the calibration zone. Calibration is normally done by displaying points in different areas around the display monitor. Number of calibration points depends on the device, calibration area and how accurate recording is required by the application. Both the pupil center and the corneal reflection is calculated at these points and a mathematical model explaining the geometry and orientation of

the eye is constructed. Naturally the eye tracker only works inside the calibrated area. Sampling rate of the device is a critical parameter for accurate tracking. Since eye movements are one of the fastest motions generated by the human body, cameras with sampling rates exceeding 250 Hz are desirable. Tracking is possible with sampling rates as low as 30 Hz but with greatly reduced temporal accuracy which does not allow measurement of saccades due to their short duration. Quality of the tracking increases with the sampling rate but seems to have diminishing gains past 300-500 Hz. High-end cameras with sampling rates over 1000 Hz are only utilized to research micro movements of the eyes, such as the jittering and microsaccades that occur inside a fixation.

Result of an IR eye tracking is a set of coordinates inside the calibrated area. These coordinate correspond the area of *acute vision* or fovea at each point as described in section 2.1. In data analysis the recorded data is often segmented into fixations and saccades (although sometimes raw data is used). In addition, eye blinks are often extracted as well to account for the time period during which the location of the eye could not be determined. This classification operation of extracting fixations, saccades and blinks is more commonly known as event detection. Various algorithms for event detection exist but most of them can be classified into one of the two categories: low-speed and high-speed. Low-speed family of algorithms examine the coordinates of the eye movement recording in terms of proximity and time [34]. These algorithms search for tightly clustered coordinates that stay clustered for a prespecified minimum time periods. These time periods are then labeled as fixations and the rest of the data transitions between the fixations are considered saccades. In some terminology low-speed algorithms are also referred to as clustering or dispersion-based algorithms. High-speed methods on the other hand calculate the velocity of the eye at any given time using the recorded gaze-point coordinates [35]. The velocity at which the eye is moving can be calculated using the equation 1 for two consecutive gaze coordinates. By analysing the velocity of the eye relative to threshold it is then possible to classify different time periods into fixations, saccades or noise.

$$v_t = \frac{\sqrt{(x_t - x_{t-1})^2 + (y_t - y_{t-1})^2}}{\Delta t} \tag{1}$$

The advantage of high-speed algorithms is the ability to detect both fixations and saccades. In doing so the information of saccade properties (amplitude, acceleration, top speed, etc) are also retrieved, while the low-speed algorithms are only capable of detecting fixations. High-speed algorithms, however, only work with relatively high sampling rates. To accurately calculate the velocity profile of the saccade sampling rate must be high enough to fully capture different phases of acceleration and deceleration. The agreed limit for reliable high-speed event detection is around 250 Hz. Low-speed algorithms on the other hand can produce reliable results with lower sampling rates.

Figure 3 illustrates the basic principle behind a velocity-based high speed event de-

tection algorithm. Left top panel of the figure contains a 3.5 second segment of eye tracking coordinate data.. Data shown here was collected during the experiment using a remote IR eye tracking camera with 250 Hz sampling rate. Below the coordinates is the velocity of the eye together with the detection threshold for saccades. This threshold is used to divide the data into fixations and saccades. Typically the speed is plotted as degrees of the visual angle over time but in this case pixels were used to keep the units uniform with the coordinate plot The bottom panel on the left shows the resulting division of the samples to fixations and saccades. On the right side of the figure the same data is plotted in two dimensions. This plot contains the sample points during the three second interval, overlaid with the detection results. This example is a simplified case and most modern detection algorithms use also additional parameters for event detection. These parameters include such variables as duration thresholds for both fixations and saccades as well as acceleration and peak detection thresholds for saccades.

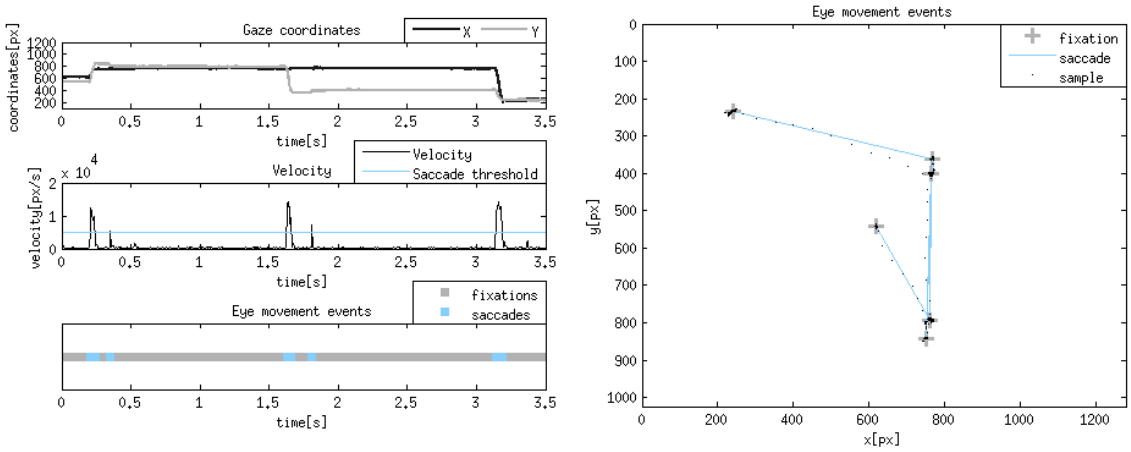

Figure 3: Example of a velocity-based event detection algorithm

2.3.2 EEG and MEG

In addition to eye movements both MEG and EEG were recorded during the experiment. Purpose of these methodologies was to capture the correlates of neural activity during a free-viewing visual search task. Both of these methods have been widely used in the field of psychological research. Advantages of MEG and EEG include their low-operating costs (compared to fMRI) and non-invasiveness. This section provides a brief background information to to the operation and background phenomenon of MEG and EEG recordings.

Electroencephalography (EEG) is a relatively old non-invasive method for studying the electrical activity of the human brain. In EEG recording, electrodes are attached to participant's scalp and the measured potentials are compared to a reference electrode. Location of the reference varies but is usually attached to either the nose, ear or some other region with very little neural activity. The electrical activity

from the scalp corresponds to the electrical activity of the brain but also contains external and physiological artifacts that have to be removed or corrected before the actual analysis. Because the measured potentials are in the order of microvolts the recorded signal must be amplified during acquisition. All modern EEG-devices store the signal in digitized format for more efficient processing and analysis. The electrical activity of the brain is based on constant firing of neurons. Due to the dampening effect of the scalp, skull and other intervening membranes between the EEG electrodes and the brain, EEG-devices lack sensitivity to detect the activity originating from a single neuron. The recorded EEG signal is in fact a spatial summation of thousands to millions similarly oriented neurons firing at the same time. A major contribution of the EEG signal comes from the post-synaptic pyramidal cells of the cortex. The main signal generator for EEG is the post-synaptic potential at the axon terminal. Due to the limited sensitivity of EEG devices the signal sources closer to the scalp are easier to observe than deep sources.

Magnetoencephalography (MEG) is another brain imaging method for recording the electrical activity of the human brain. MEG is based on recording the very weak magnetic fields (in the region of 0.5 pT) generated by the neuronal currents. More specifically the detected field is induced in the dendrites of the neurons during a synaptic transmission. The recorded signal shares characteristic with the EEG signal but there are benefits of recording both signals at the same time. Detection of these magnetic field is possible through the highly sensitive *superconducting quantum interference device* (SQUID) sensors. Typical MEG devices contain two types of SQUID sensors: magnetometers and gradiometers. Magnetometers are used to sense the magnitude of the perpendicular magnetic field while the gradiometers pick-up the spatial gradient of the field. Using a set of three sensors (1 magnetometer and 2 gradiometers) for each sensor location it is possible to thoroughly record the magnetic field of the underlying signal. In order to function the MEG device requires a magnetically shielded room as the recording is very sensitive to outside interference. Unlike EEG, the MEG is unable to detect radial sources and is only sensitive to tangential currents which makes the simultaneous recording of EEG and MEG especially appealing for source localization [36].

2.3.3 Co-registration

Eye tracking is exceptionally useful when paired with brain imaging methodologies. In the past eye trackers have been used in research with EEG, MEG and fMRI. Addition of eye-tracking benefits the research of visual EEG/MEG in two ways.

1. Eye tracking provides information regarding the visual input at each of the recorded time points.
2. Eye tracking enables the removal of EOG artifacts by dividing the EEG/MEG data to fixation-locked segments.

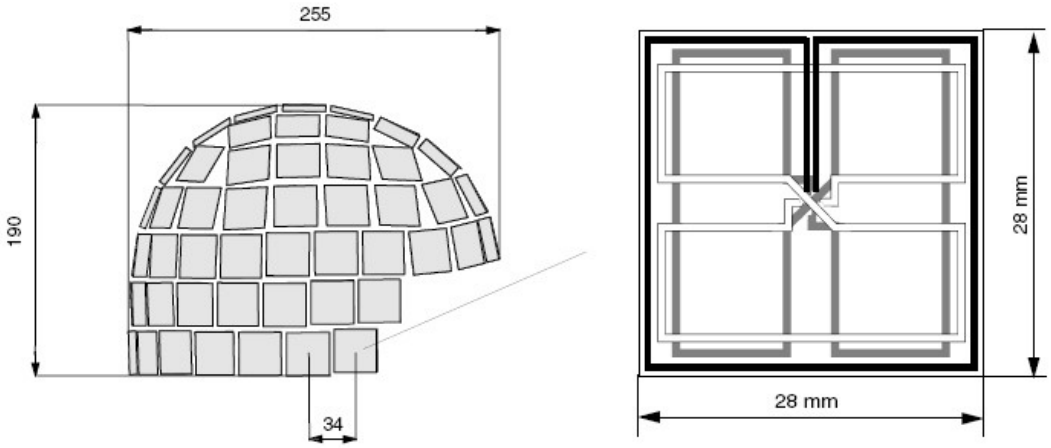

Figure 4: MEG sensor layout and the structure of a single sensor unit [37]

In the case of visual stimuli the combination of the two methodologies allows the researchers to accurately determine both the visual input as well as the neural response. Eye movements can be used as natural and self-paced markers to segment the EEG/MEG data into meaningful time-epochs. Co-registration also enables the use of free-viewing setups. As mentioned earlier in section 1 the EOG activity in both EEG and MEG recordings was traditionally considered an artifact. This is due to the electric activity of the eye movement (caused by eye being a natural dipole) having the tendency to mask underlying EEG activity. Numerous methods exist to estimate and correct ocular artifacts from a recording [38] [39]. The inherent problem with these methods is the risk of removing actual data along with the artifacts. Co-registration of eye movements and EEG/MEG provides a new solution for the problem. With a concurrent eye tracking recording it is possible to either limit the analysis of the EEG-signal into time windows during which the eye was in a fixation. This technique is known as fixation-locked potential or fixation related potentials. Other methods use eye movement data as an additional data signal to perform the artifact correction. These methods allow the use of free-viewing experimental setup where eye movements no longer critically hinder the data analysis [40].

An inherent problem with adding new recording modalities into an experiment is the synchronicity between devices [41]. Co-registration only works if all of the three recording devices are operating under the same clock. The problem arises from the fact that each recording device has its own internal clock which controls the operation of the device. The internal clocks differ slightly but even a non-systematic time difference of 10 milliseconds can render the analysis impossible. Furthermore the slight differences between the clocks tend to amplify in long recordings through a process known as *clock drift*. For this reason asserting and correcting synchronicity is a mandatory step in co-registration paradigms. In most acquisition devices the recorded data also contains a time-stamp for each sample. With these timestamps the different recordings can be synchronized as a post-processing step as long as

each recording contains mutual trigger signals. To generate mutual trigger signals an external computer is often used for stimulus presentation and triggering. This computer displays the stimuli and sends trigger signals to each of the acquisition devices which then encode the trigger signal in the data stream. One way of synchronizing multiple recordings is to adjust the temporal properties of one or more of the signals through interpolation. An alternative approach is to analyse the data in short segments around the trigger signals where the internal clocks of the different devices can be considered to be in synchrony. In this experiment the latter method was used.

2.4 Event related potentials

2.4.1 Event related potential technique methodology

The methods of analyzing the EEG signal vary based on the application. In clinical diagnostic applications, such as medical devices that measure the depth of anesthesia [42], metrics derived from the power spectrum are commonly used. In spectral analysis of EEG the signal is first transformed into the frequency domain and power modulations of different bands and electrode locations are analysed. In brain research, spectrum-based analysis methods are also used but it is more common to examine EEG in time-domain as event related potentials (ERPs) [43]. The basis of ERPs is the temporal averaging of repeated measurements in order to discover a specific underlying waveform related to the task or stimulus. ERPs can be described as phase-locked oscillations of a specific cluster of neurons, strong enough to produce a detectable waveform through averaging. Because EEG has both stochastic and deterministic properties the recordings generally contain a lot of activity not directly related to the investigated phenomenon. To extract the ERP from the background noise, multiple repetitions of the task or stimulations is required in order to make the waveform visible. The exact number of repetitions depends on the robustness of the neural response being investigated but the signal-to-noise ratio of ERPs is generally considered to follow the square root of the number of trials [44]. Purpose of the ERP technique is to discover latencies, amplitudes and shapes of the different responses and how these relate to the used stimulus or task. Various statistical tests are also employed in order to assert that the obtained waveforms are statistically significant.

ERPs have been studied for a very long time and a comprehensive report can be found in [44]. The result of ERP research is a precise taxonomy of different neural responses. In ERP literature different responses are noted using a prefix N or P. The prefix indicates the polarity of the response, where N stands for negative and P for positive. The prefix is followed by a number which indicates the typical latency of the ERP. For instance P300 ERP is an ERP with a positive polarity which occurs around 300 ms after the presentation of stimulus. Depending on the literature the latency might be truncated to just hundreds of milliseconds (such as

P3 in psychological literature regarding the potential). It is also worthy to note that in some literature the polarity of the responses is plotted in downwards direction for historical reasons. Here, however, all ERPs are plotted with positive polarity pointing upwards. ERPs have been used to study various neural processes such as auditory, visual and even some BCI applications. In the analysis of ERPs the signals are often low-pass filtered with a 30 Hz cutoff filter in order to further minimize noise and clarify the shape of the response. [44]

2.4.2 Visually evoked potentials

Neural responses resulting from processing of visual information are known as visual (event-related) potentials. ERPs that relate to visual stimuli and are recorded from the occipital lobe are called visually evoked potentials (VEPs). VEPs are used in study of attention and other psychophysical experiments regarding visual inputs. In clinical diagnostics they are also used to diagnose multiple sclerosis by inspecting the functionality of the visual pathway [45]. In vision research the two most prominent visually evoked potentials are the C1 and the P1 potentials. P1 is named according to the typical ERP taxonomy where P signifies positive polarity and the 1 indicates the typical latency in hundreds of milliseconds. P1 peak is a positive potential that peaks around 100 ms after visual stimulus onset. P1 is omnipresent result of visual sensory stimulation and is not directly task-dependent. P1 amplitude has been shown in some cases to be influenced by top-down factors [46] but is typically considered to consist mostly of the low-level features of visual stimuli such as luminance [47], contrast and edge density [48] of the visual input. The signal generator for the P1 response is located in the dorsal extrastriate cortex which in the typical 10-20 EEG montage lands in near the center of the occipital electrode site. A second early visual response is the peak of the C1 wave. C1 wave is a visual potential with a varying polarity which is influenced by the location of the stimulus in the visual field. C1 occurs between 50-100 ms after fixation onset.

In addition to visual input, some VEPs are also generated by the neural correlates of saccades [49] [50]. Lambda response is a saccade related potential occurring approximately 80 ms after saccade-offset. Earlier studies have found lambda response to correspond to preceding saccade parameters but stimulus control experiments have shown that it can also be modulated by visual inputs [51]. Source localization of the lambda response indicates that it has common neural generators with the P1 response. Another saccade related potential is the saccadic spike potential (SP). According to existing research the SP is caused by the recruitment of motor neurons required to complete the saccade [52]. Source localization places the origin of the SP around the central and parietal regions of the brain [53] [54] and studies of the SP latency indicate that it peaks several milliseconds after the saccade onset [50]. Lambda response and the spike potential indicate that both low-level visual properties of the perceived visual stimuli as well as the oculomotor properties modulate the amplitude of the early visually evoked potentials.

It is plausible that what is typically labeled as P1 can in reality be caused by a combination of the aforementioned components. In this article separation between various sources is omitted, instead all VEP components are clustered into a single measurable parameter. This method could be considered a black-box approach where the human visual system in a free-viewing paradigm is investigated in a data-driven manner to discover how the visual input and the oculomotor properties modulate the amplitude of the recorded potentials.

In figure 5 all fixation-locked segments of EEG collected during the experiment were averaged over subjects and plotted as a time-series in the lower panel. In this plot time point zero corresponds to the offset of the preceding saccade and beginning of the fixation. Channels located on the occipital lobe (O1, O2 and Oz) were colored blue as the effect is most visible on these channels. From time-series the early visual responses are clearly visible from 50 to 100 ms post-fixation onset with a peak around 75ms. Above the time-series are three topography plots from three time-points (25, 75 and 175 ms) which demonstrate the spatial distribution of the EEG amplitudes. Also visible in the figure is the negative N1 deflection wave around 125 ms. This VEP is also result of visual processing but is outside the scope of this thesis. This figure also clearly demonstrates the variation of VEP amplitudes and waveforms (and in truth all ERPs share this characteristic) over individual subjects.

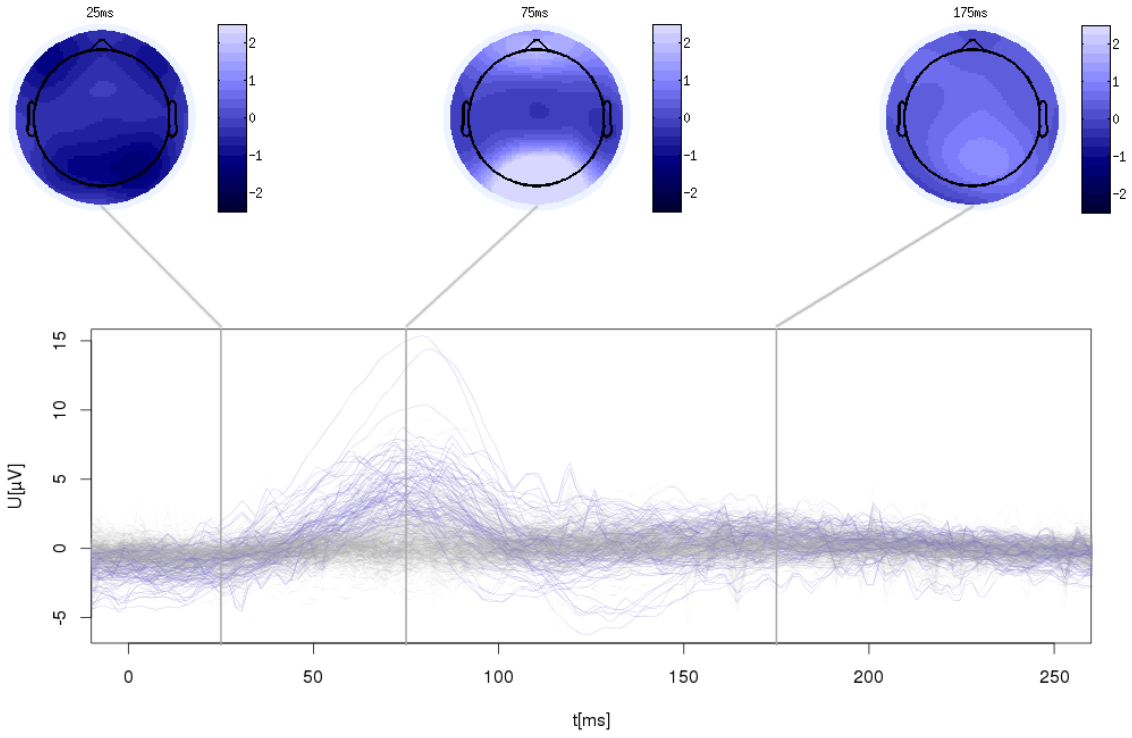

Figure 5: Visually evoked potential as a time-series with topograhpy plots from three time points (25, 75 and 175 ms)

2.5 Linear Mixed Effect Model

The overall aim of the experiment was to record EEG during a free-viewing of natural stimuli. The collected EEG is then processed and segmented according to fixations occurring in each trial. These fixation-locked segments are then further analysed with a statistical modeling technique called linear mixed effect modeling (LMM). The purpose of the model is to explain the amplitude of the early visual response in different locations of the scalp as a function of various parameters including variables from visual input and saccade kinematics. This section provides the mathematical theory behind this model and the details about applying it to the data. Parameter selection for the model is also discussed, although more detailed description can be found in section 3.5.

Linear mixed effect model (LMM) is a multiple regression model that explains a dependent variable $\mathbf{y}$ in terms of linear regressors (called fixed-effects in this context) $\mathbf{X}$ and random effects $\mathbf{Z}$. In practice LMM is very similar to regular linear regression with the exception of the random effects term. In LMM fixed-effects correspond to factors that are known to have or are suspected to have influence on the dependent variable. Mixed-effects on the other hand are variables that are known to cause random and uncontrollable variations in the dependent variable. Equation 3 presents the LMM equation in matrix form. For comparison the matrix form equation of linear regression is presented in equation 2.

$$y = \boldsymbol{X}b + \epsilon \tag{2}$$

$$y = \boldsymbol{X}b + \boldsymbol{Z}u + \epsilon \tag{3}$$

Values for the parameters of the linear mixed model are calculated using the maximum likelihood (ML) estimation. When sample sizes are small ML estimation can be biased in the estimation of the variance components. When dealing with small sample sizes it is also possible to use restricted maximum likelihood estimation (REML) [55] to compensate for the bias.

For the model to be valid the fixed-effects variables must satisfy certain conditions [56]. First assumption is that all dependencies of the underlying phenomena should be linear in order to fit a linear model. This assumption can be verified by examining the residuals of the model. Second assumption is that different fixed effects of the model should not be linearly correlated. Correlated fixed effects undermine the stability of the model. Collinearity of fixed effects can be assessed by computing correlations between all of the fixed effects. Third assumption is that residuals of the model should also be evenly distributed over the fitted values. Even distribution indicates that variance over the model is uniform (i.e. the "credibility" of the model does not change through the course of the fitted values). Fourth assumptions is that the residuals of the fitted model should also be gaussian. Finally the fifth assumption dictates that each of the samples fed into the model are independent (i.e. from an unique source). As most experiments of this type consist of repeated

measures this assumption is impossible to satisfy. Instead this can be compensated by adding subject as a mixed effect to the model. [57]

In statistical modeling a model that accurately describes the response of interest with fewest possible parameters is preferred. It is reasonable to start with a full-model consisting of all possible variables that fit the theory. After formulation of the full model the best approach is to reduce the model to minimum amount of parameters that best explain the data. Kullback-Leibler distance (KLD) is a metric used to describe the informational distance between two probability distributions. One way to interpret KLD is the information lost by forcing the data into a specific model. It thus follows that the minimization of the KLD produces the optimal model for the data. The most prominent model reduction technique based on KLD is the Akaike Information Criterion (AIC) [58] [59] which can be found in equation 4.

$$AIC = 2k - 2ln(L) \tag{4}$$

In equation 4 k is the number of predictors in the model. The number of predictors is used to penalize the AIC score as models with large numbers of predictors (or fixed effects in the case of LMM) tend to have higher maximum likelihood values. AIC can be used to select the best fitting model from a set of models by minimizing the AIC score. A common way of applying AIC is to use a step-wise backwards selection where predictors are dropped from the model in an attempt to minimize the AIC score. The resulting curve of AIC scores should indicate which fixed-effects are most relevant for the model.

Multiple different methods exist for quantifying the statistical significance of linear mixed effect models. These methods range from bayesian inference to regular analysis of variance based (ANOVA) test. In this experiment the statistical significance of the produced models were assessed using a likelihood ratio tests (LRT). LRT is based on forming two models: the actual model of interest and a null model. The actual model is the resulting model of applying LMM. The null model is a reduced version of the actual model containing only some (or in the extreme case none) of the fixed effect variables. The test statistic D is defined as a logarithmic ratio of the likelihood functions of the two models.

$$D = -2ln(L_0) + 2ln(L_1) \tag{5}$$

In this experiment LRT was used to determine statistical significances. Likelihood-ratio tests, however, only work with models that have been estimated using ML instead of REML. For this reason the models were also calculated using ML.

3 Materials and methods

3.1 Experimental design and implementation

The experiment conducted in the TEVSOC project was a simple visual search task. A dataset of 70 greyscale nature photographs selected from the DOVES database [60] were used as the stimuli. The selected photographs contained only forest sceneries with no man-made objects or people in them. Purpose of this selection was to assert that the picture dataset was semantically homogeneous. Histograms of all the selected images from the dataset were matched to the mean histogram of the entire image set. To preserve original structure of the images a structural similarity index (SSIM) algorithm [61] was used in the matching process. Images were normalized in MATLAB using the SHINE toolbox [18] with SSIM option for the preservation of the original structure. The resulting dataset of images was thus normalized in a global sense while still having local differences. The experiment included three stimulus conditions: natural, scrambled and control. In the natural condition the image was unaltered except for the histogram matching. In the scrambled condition the image was divided into an equispaced 4 x 4 grid and the order of the grid elements was randomly scrambled. To control the strong contrast differences arising from the scrambling, images in the both natural and scrambled condition were overlaid with a 4 x 4 grid consisting of 2 pixel wide black lines. The third control condition consisted of a solid gray color which with the black grid overlay. The color of the image was set to the average pixel value of the image dataset. Image scrambling is a method which has previously been used to investigate the effect of top-down processing in a visual search task. [62] The purpose of the two primary stimulus conditions (natural and scrambled) was to generate situations where either top-down or bottom-up processing was more imminent. In the case of the natural stimulus the semantic information of the photograph is present. It is thus logical to assume that attention in the natural condition is controlled more by top-down mechanism. In the scrambled condition semantic information is distorted and in this case the test hypothesis was that attention is controlled by bottom-up mechanisms based on visual saliency. Example of each stimulus condition can be seen in figure 6.

Figure 6: Stimulus conditions: natural, scrambled and control

Experiment consisted of a total of 210 trials equally divided among the three conditions and each of the trials had the same task. In each trial the subject was first

presented a small image patch called a target. All of the targets were the size of a single grid element of the larger stimuli. Furthermore all targets have been selected from the elements of the larger images. Target patches were selected through a clustering analysis of all the patches within an image. Purpose of the clustering analysis was to pick most distinct target patches for each trial. Target patches were also uniformly distributed over the 16 possible locations in all task conditions. The subject viewed the target for 4 seconds after which a full-sized scene picture of one of the three conditions was displayed. The subject was allowed to examine the scene picture for 8 seconds. After 8 seconds the subject was asked if the presented target was part of the larger image. Display times of both the target and the full image were based on results from a pilot study conducted to discover typical response times for the task. Subjects delivered their answer in yes/no format using an optical response box. Between each trial the subjects focused on a fixation cross on the center of the screen. The duration of the fixation cross was randomized in order to prevent anticipatory effects. The experiment was divided into 5 blocks in order to counter the fatigue factor. The presentation order of the blocks was varied over the subject in order to counter balance the experiment. Between blocks the subject was allowed to rest and the eye tracking camera was re-calibrated before the start of the next block. Stimulus presentation and synchronization of the recording devices were implemented using Presentation-software. Structure of a single trial is visualized in figure 7.

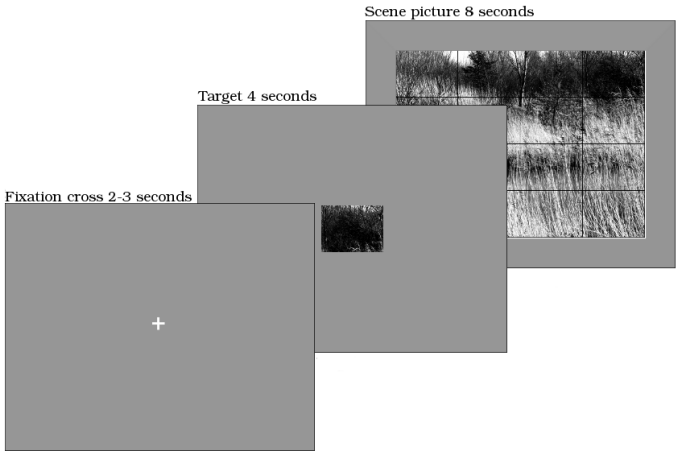

Figure 7: Structure of a single trial and display durations of each component.

3.2 Acquisition

3.2.1 Apparatus

EEG and MEG were recorded using a Elekta Neuromag VectorView device. The EEG system consisted of a 60 unipolar channel EEG cap (EasyCap) with 78 Ag/AgCl sintered ring electrodes. The reference electrode was placed on the tip of the nose.

Four additional bipolar (differential) electrodes were attached around the eyes in order to register the electrical activity caused by eye movements. EEG electronics were located inside the MEG gantry and connected to the cap through two 37 pin male headers. In addition to the header the EEG interface had separate sockets for ground and reference electrodes as well as the bipolar electrodes. EEG electronics consisted of a preamplifier and Signal Acquisition Board which handled the digitization of the recorded signal. After the EEG cap was adjusted to the participant's head, the locations of all the channels were registered using the Isotrak 3D digitizer. The MEG device consisted of 204 planar gradiometers and 102 magnetometers. The sensors were positioned in the manner described in section 2.3.2. Thus each of the sensor location had one magnetometer and two orthogonal planar gradiometers. The MEG gantry supports recording in both supine and seated position. In the experiment all the measurements were conducted using the seated position. Both EEG and MEG were recorded at a 600 Hz sampling rate. Both data streams were saved on file without applying any filtering or averaging. The recordings were saved in Elekta's proprietary FIFF-format. Layout of the EEG sensors can be seen in figure 8 and MEG sensors in figure 9.

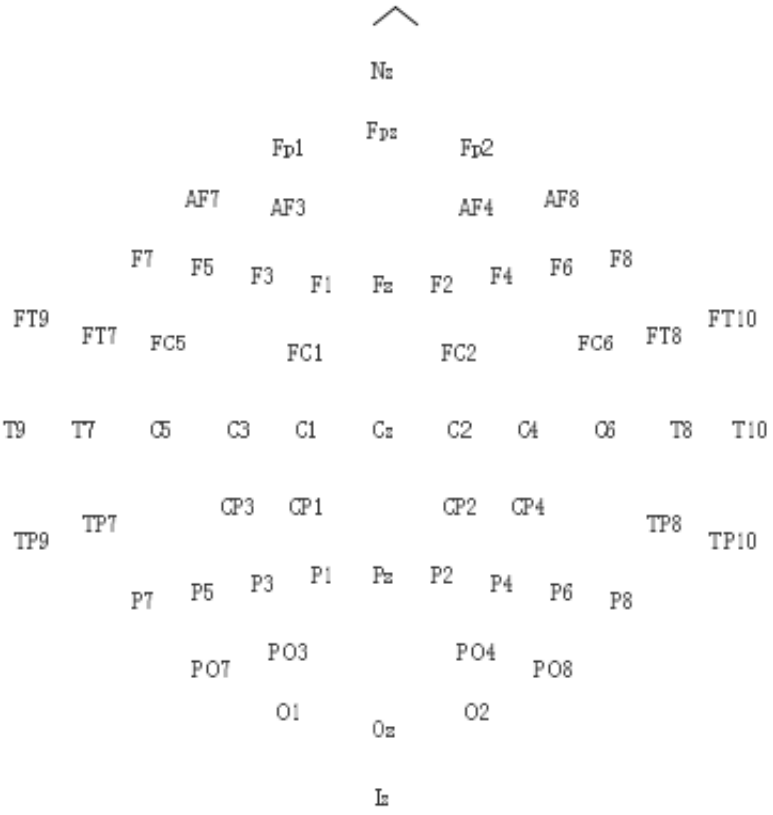

Figure 8: EEG sensor layout

The head location inside the MEG device was registered and monitored through head position indicator (HPI)-coils. In the experiment 4 HPI coils were placed in

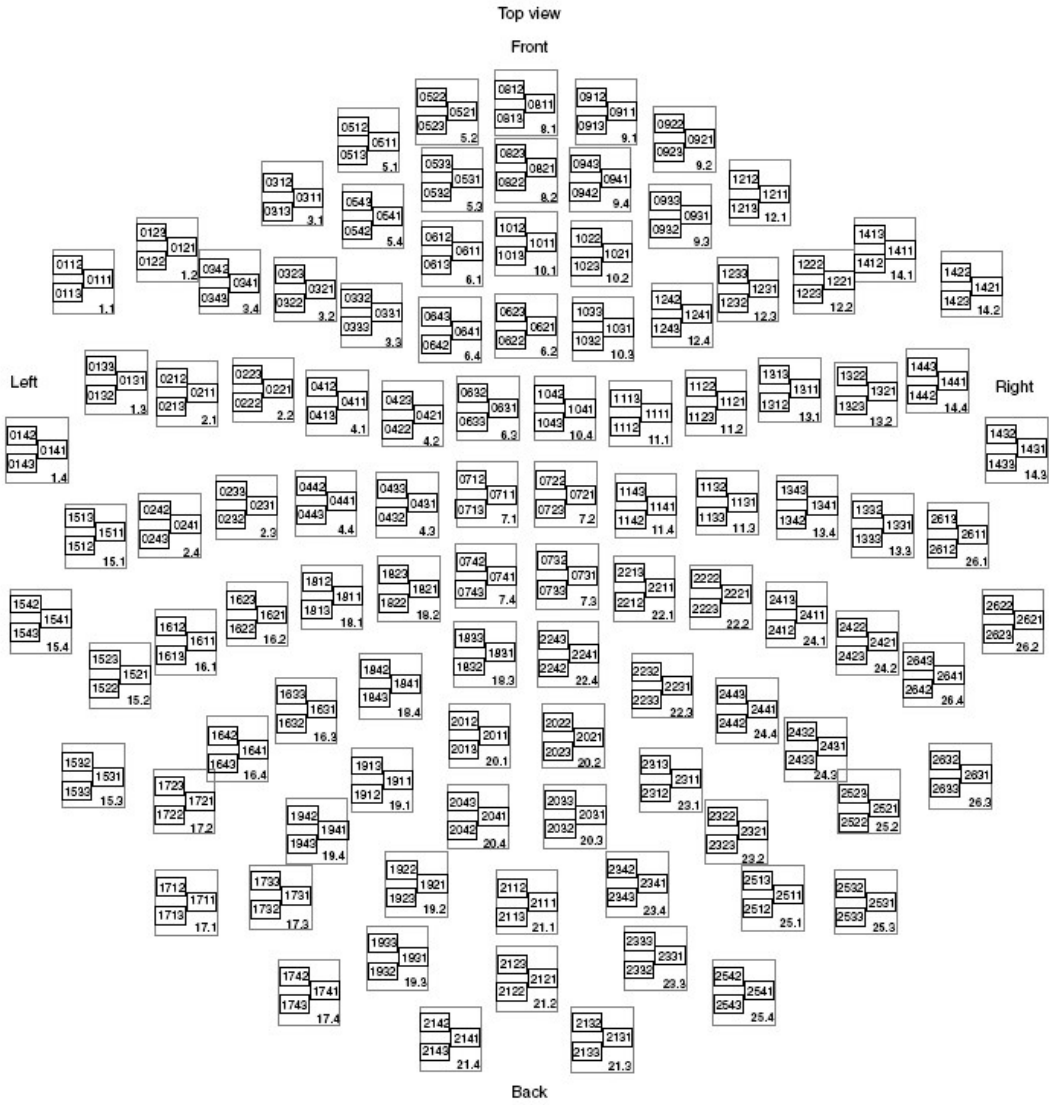

Figure 9: MEG sensor layout [37]

a equispaced circle around the subject's head. HPI and the digitized anatomical landmarks are used to align subject's head with the device coordinate frame. In other words this procedure connects the data acquired by the device to a specific anatomic location. This information is necessary for source modeling. HPIs can also be used for continuously monitor the head position inside the device but this feature was not used in the experiment.

Eye movements were recorded using the SensoMotoricInstruments remote iViewX MEG250 eye tracker. The tracker was MEG-compatible and thus presented no external artifacts to the recorded signals. Device itself was a tripod mounted camera with a circular IR light source attached to a boom arm. The eye tracker was used for recording eye movements from a the right eye of each subject. Sampling rate of the device was 250 Hz and the signal was recorded using iViewX-software running on

a separate computer. The device used a oval fitting method for detecting the pupil and thresholding for the cornea reflection detection. a 9-point calibration sequence was used to setup the device.

Data acquisition was performed inside a magnetically shielded room (ETS Lindgren, Euroshield Ltd.) and the stimulus was presented on a screen in front of the subject using a back projecting display screen. The projector used to display the stimuli was a digital light processing (DLP) projector. The distance between the screen and the subject was roughly 1.5 meters. A photograph of the measurement setup with the subject inside the MEG gantry can be seen in figure 10.

Figure 10: Recording apparatus

3.2.2 Quantifying the spatial accuracy of the eye tracker

At the beginning of each experiment block the eye tracker was re-calibrated. The eye tracking camera had no way of saving the calibration information or an estimate of the calibration accuracy. For this purpose a spatial accuracy test protocol was implemented to save calibration quality and it was executed at the beginning of each experiment block. The test protocol consisted of displaying 16 crosses on the

screen in a randomized sequence. The display time of each cross was adjusted to one second so that the subject had enough time to fixate each cross once. The locations of the crosses corresponded to the grid centers of the 4 x 4 overlay used in the actual stimulus. These locations were selected as they were considered to be a good estimate of the region where calibration should be accurate. After performing event detection to the eye movement data it was then possible to quantify the calibration error of the device in these 16 locations. For each location the coordinate offset and dispersion of the fixation were calculated and stored. These values were later used to reject badly calibrated EEG segments from the dataset. The order in which the crosses appeared was randomized on each run to prevent anticipation. Figures 11 and 12 illustrate the results of a successful calibration and a poor calibration. In these pictures black cross marks the location of the displayed fixation cross. Gray X-symbols correspond to the registered fixation locations and the average dispersion in x- and y-directions is displayed as a circle. The numerical value for the offset in pixels from the target is also written next to each fixation.

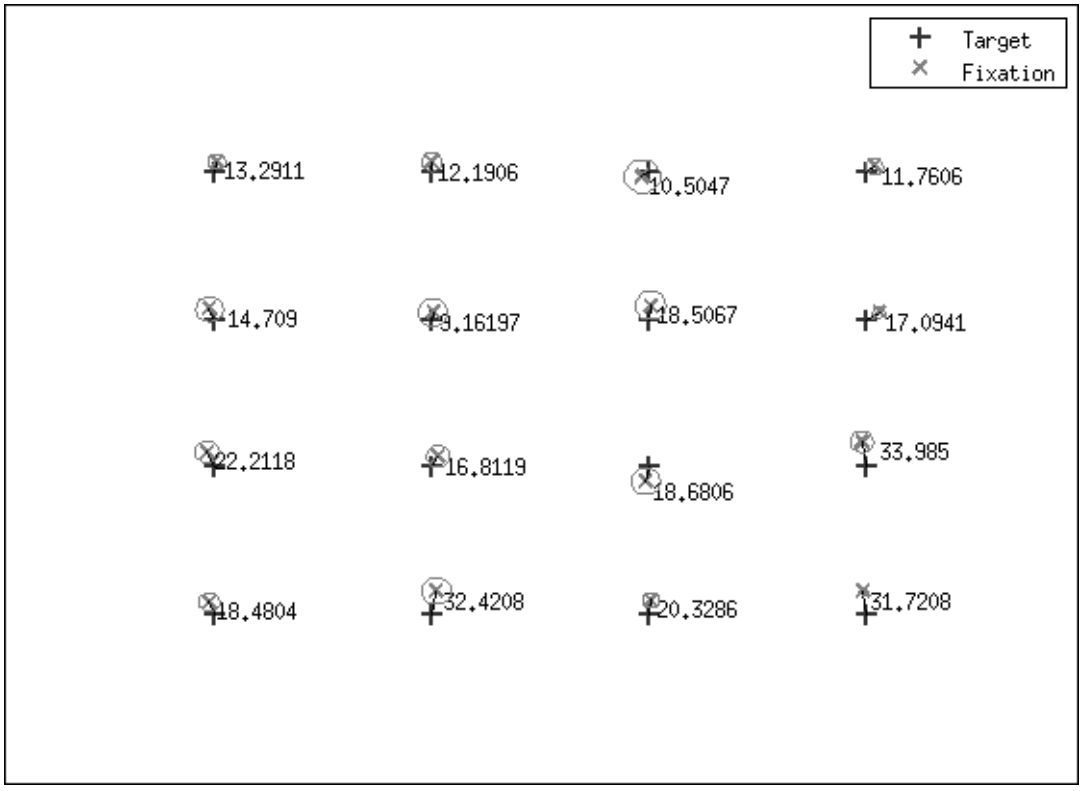

Figure 11: Result of a successful eye-tracker calibration

3.2.3 Temporal synchronization of the acquisition devices

For accurate application of the co-registration technique temporal synchronicity must exist between the devices. In the ideal case both the MEG/EEG and eye tracker would be running under a single clock. Unfortunately each device has their

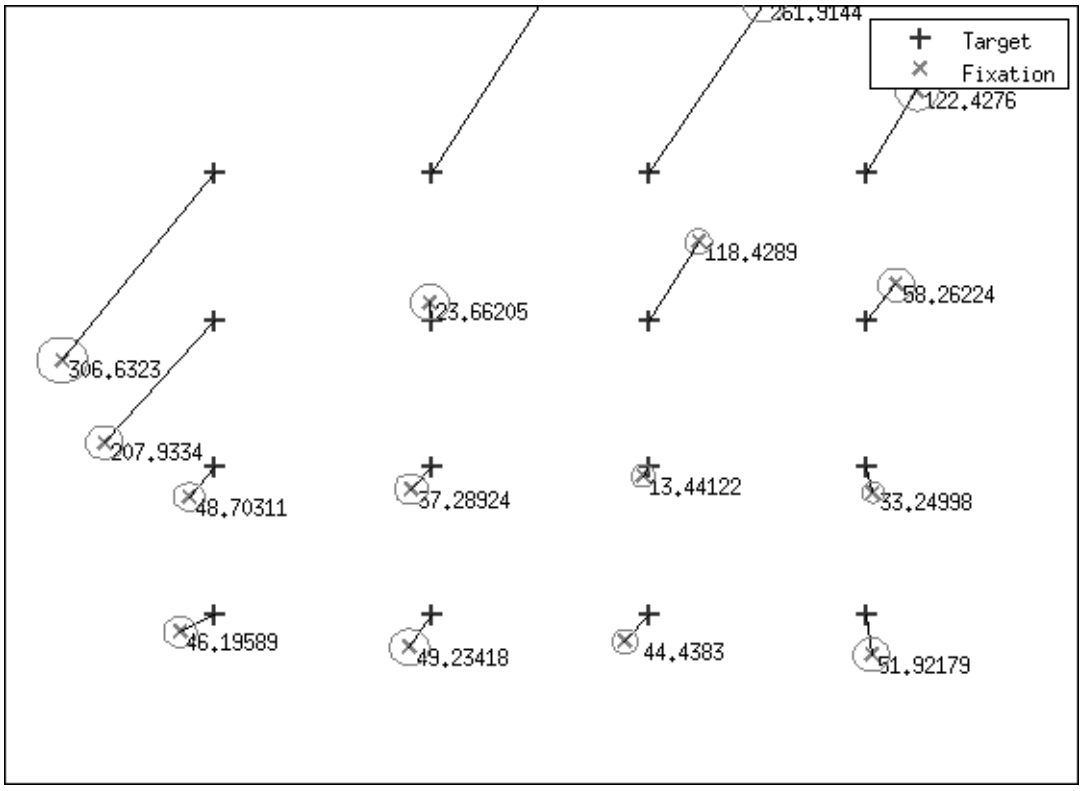

Figure 12: Result of a poor eye-tracker calibration

own internal clock and it is also wrong to assume an ideal condition where the two independent clocks would operate at the same rate. Synchronizing the devices in real time is difficult so an alternative approach was used. The stimulus presentation computer was capable of transmitting triggering signals to both data streams. In the case of MEG/EEG the communication protocol was 4-bit TTL pulses sent through a parallel port. On the eye tracker side the communication was over an Ethernet protocol. The experimental setup was configured to send mutual messages to both data streams which were later used to synchronize the recordings offline in the preprocessing stage of the data analysis. Due to two different communication protocols (TTL and Ethernet) the latencies of triggering messages were also different. It is possible to compensate this difference by first measuring the average latency for both protocols and then modifying the timestamps of the triggering signals as a post processing step. In this experiment, however, there was no need to correct for latency as the time-window for EEG segmentation was determined from the data. As such it was not imperative to know the exact latency of the two triggering protocols as long as the latency in both triggering streams remained relatively stationary. This assumption was tested by calculating the average variation between two triggers in both cases. The average jitter in both systems was approximately 1 ms which was within acceptable limits for synchronization purposes. More details on the synchronization procedure are in section 3.4.

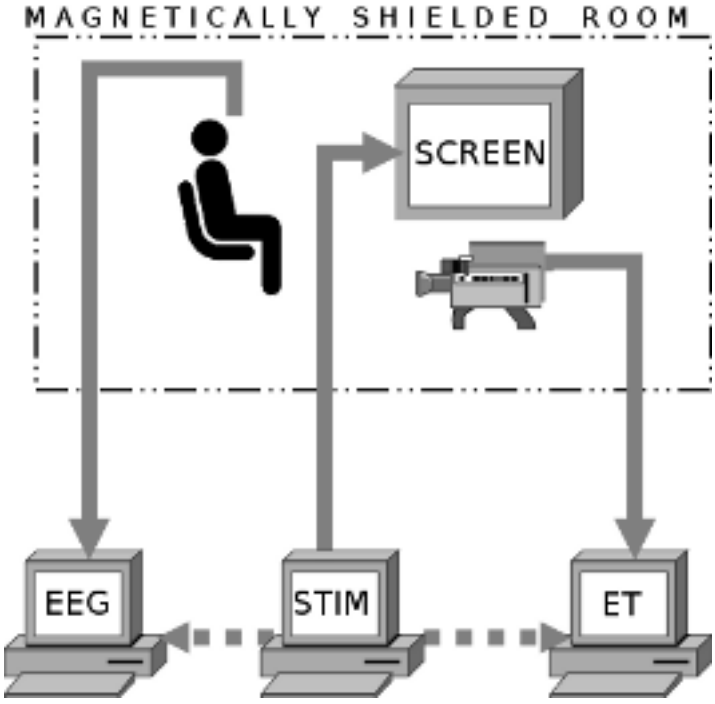

Figure 13: Setup for synchronizing multiple measuring devices

3.3 Procedure

This section describes a typical recording session. The total number of participants was 32 out of which 28 were used for the actual analysis. Each subject had normal or corrected-to-normal vision, no diagnosed neurological or psychological deficiencies and used no medication which affects the central nervous system. The duration of a single recording session was between 1.5 to 2 hours. Most of the participants were student volunteers recruited through mailing lists. Rewards for the participations was 5 culture tickets (worth 5 euros each). Steps of a typical recording session are listed below.

1. Arrive at the recording site and test MEG equipment. This consisted of visually checking that all the channels were working properly during an empty room recording. Channels with spurious activity where either reset or heated in order to solve the problem. If a particular channel could not be made functional it was marked down in the measurement journal. Optical response box and TTL pulse triggering channels were also inspected at this point.

2. When the subject arrives they are first given a brief introduction about the experiment. Subject is then asked to read the written instructions about the experiment and sign a consent form.

3. Subject was briefed about the magnetic sensitivity of the MEG device. Subject was then instructed to remove all metallic objects from their body (jewelry, hair pins, watches, etc). If subject had clothes that included metal parts

(zippers, studs in jeans, etc) they were instructed to change those items to provided hospital garbs. Subject was also asked to remove any make up around their eyes. Reason for this was two fold. Firstly the eye mascara can contain metal particles which during blinks and eye movements can cause distortions in the recorded magnetic field. Secondly black eye mascara deteriorates the eye tracker calibration quality when attempting to localize the pupil. If the subject had glasses they were replaced with MEG compatible plastic glasses of equal prescription for the duration of the experiment.

4. After subjects were considered MEG compatible they were prepared for EEG. This included fitting a EEG cap on the subject and preparing the electrode sites. Each electrode site was first scrubbed with a q-tip in order to push hair away from the scalp. Gentle scrubbing also reduces the contact impedance as the area is cleansed of dead skin cells and dirt. After scrubbing the EEG electrodes were filled with conductive EEG gel.

5. HPI coils were attached on the EEG cap with scotch tape. Coils were attach high enough so that they would fully enclosed inside the MEG dewar and thus present a clear signal for the device.

6. Anatomical landmarks, locations of the HPI coils and all of the EEG channels were digitized using the Isotrak 3D digitizer. Procedure was started by activating the registration sequence from the user interface of the MEG device and then pointing out anatomical locations, HPI coil locations and EEG channels with a digitizer pen.

7. Subject moved inside the magnetically shielded room and seated inside the MEG gantry. Wires from the EEG electrodes were connected to the signal acquisition board. The seat of the MEG gantry was raised so that the subject's head was fully inside the dewar. Subject was also instructed about the task at this point.

8. Electrode contact impedances were measured from the EEG and corrected if necessary. Electrode contacts were improved until all electrode impedances were near or below 5kΩ

9. Subject was given the optical response and instructed how to use it. Subject was to lift their thumb for *yes* and index finger for *no*. At this point the optical response was tested once more.

10. Eye tracker was set up on a tripod mount in front of the subject. The lens of the camera was aligned towards the right eye and the IR illuminator was adjusted until both the pupil and cornea reflection were detected by the camera. In cases where detection of the cornea reflection was poor the focus was offset to generate a sort of low-pass filter for more stable image.

11. Back projecting screen was brought into the magnetically shielded room and placed in front of the subject. DLP projector was turned on and image quality was checked.

12. Head localization using HPI coils and the automatic software was used. If the HPI check failed the position of the HPI coils was changed. The recorded head position coordinates were saved for further use.

13. Eye tracker was calibrated using a 9 point calibration sequence. In the case of calibration failure or poor data quality after calibration the eye tracking camera was readjusted.

14. The experiment was now ready to be ran and the first block could be started. Recalibration of the eye tracker and other modifications to enhance the signal quality were performed between each block. Collected MEG, EEG and eye tracking data were saved on file after each block. During each block the subject was monitored through a video camera and a two-way intercom was also used to communicate with the subject.

15. After 5 blocks the subject was free to exit from the magnetically shielded room. Subject changed back to their own clothes and were given a reward of 5 culture tickets.

3.4 Preprocessing

Before the actual analysis the data was subjected to various forms of preprocessing to remove all possible noise from the signal. First step of the preprocessing chain was to run the collected data through a MaxFilter-software. MaxFilter is part of the Elekta Neuromag software package and is used to suppress outside magnetic interference from the recorded biomagnetic fields. MaxFilter can also be used to compensate for head movements using the data from the HPI-coils but this step was omitted in the preprocessing chain. Head movement compensation runs the risk of distorting the data and should not be applied without compelling reasons (i.e. subject unable to sit still due to epilepsy). MaxFilter was used to perform Maxwell filtering [63] (named after Maxwell's equations on which the method is based) for the recorded data. In this operation the data is decomposed into three components by utilizing signal subspace separation. These three components are signals originating from inside the brain, external disturbances and noise generated by sensors or sources with close proximity to the sensors.

In the second stage the data was loaded into BESA-software. An adaptive noise removal algorithm [64] was used to remove ocular artifacts from the data. In this method ocular artifacts were first identified visually from the data. Visual identification was possible due to the distinct wave form of ocular artifacts caused by saccades and blink. In addition the bipolar EOG channels made identification easy. A data segment consisting of purely eye movements was used for this step to reduce the chance of removing components of interest. The segment used for this purpose was the calibration accuracy test explained in section 3.2.2. For this purpose eye movement components were defined outside the task trials. BESA computes a principal

component analysis (PCA) using the marked EEG segments in order to generate a model of the artifact which is then applied to the rest of the data.

In the third stage the eye movement data was first synchronized with the MEG/EEG recordings using the mutual trigger codes saved during the recording. In this stage the original trigger channel from the MEG/EEG recording was first exported from BESA and then loaded into MATLAB along with the triggering information from the eye tracker recording. Synchronization was based on the assumption that the clocks of the two recording devices (MEG/EEG and eye tracker) could be considered to operate at an equal rate in small time windows. In other words, processing the data in small segments around shared markers would cause the data to be synchronized. It was reasonable to assume that drifts between the devices only occur in longer time periods. The shared triggers used in synchronization were the markers which indicated the beginning of each trial. After synchronization the eye movement data was used to segment the MEG/EEG recording according to fixation onset times occurring while viewing the large scene picture. Event detection of the eye tracking data was performed using the high-speed event detection application from the manufacturers software package (SMI iTools). The software package contained SMI's implementation of an existing event detection algorithm [65]. Parameters used for detection were 50 deg/s threshold for saccade velocity and a 50 ms minimum duration for fixations.

EEG was segmented into time epochs based on the fixations found in eye tracking data. Time epochs were 500 ms in duration starting 200 ms before the onset of the fixation. Resulting EEG segments were baseline corrected by subtracting the mean amplitude value of each segment. In addition, each segment was also band-pass filtered to frequency range of 0.5 to 30 Hz using a zero-phase digital filter. As a final step, the EEG segments were pruned by inspecting the recorded potentials inside each segment. Segments containing potentials that exceeded 120 uV were rejected. Also segments which belonged to a recording with unsatisfactory calibration quality were discarded. Rejection was based on thresholding the calibration accuracy values collected at the beginning of each block. Fixations that were registered in a location with poor calibration accuracy or large dispersion were removed. Threshold for removal was 80 pixels in both calibration offset and dispersion. Resulting loss of data for both rejection methods is displayed in figures 14 and 15 The resulting fixation-locked single trial EEG data segments exported from BESA were then used in the statistical analyses to form the LM-models.

3.5 Statistical analysis of the collected data

3.5.1 Outline of the analysis

Purpose of the statistical analysis was to first construct a model describing the generation of the early visual potential as a function of low-level visual input and oculomotor variables. After a reliable model has been generated the effect of top-

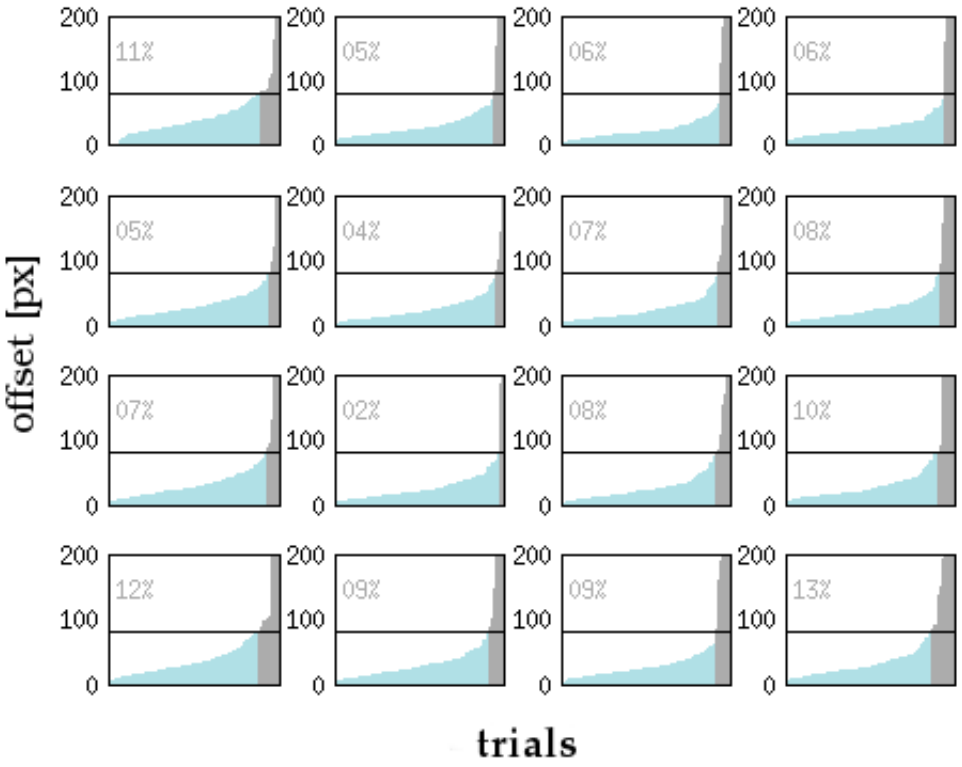

Figure 14: Portions of rejected data marked in grey in 16 grid locations based on the calibration offset

down processing can be investigated by inserting stimulus condition (natural vs. scrambled) as an additional fixed-effect variable. Starting point for the analysis was the 500 ms segments of EEG data resulting from the preprocessing chain of chapter 3.4. Note that even though both EEG and MEG data were collected in the experiment, only EEG data was used for the statistical analysis at this stage. The rationale behind this decision was to first formulate the model as channel-based and later expand it to cover the actual neural sources localized using the MEG data. The EEG-only approach was also selected as to make the results comparable to earlier EEG-based studies of the early visual potentials. The source based LMM analysis of the MEG data is beyond the scope of this thesis but it is briefly covered in section 6. The statistical LMM analysis was implemented in R [66] using lme4 [67] package.

In order to model the generation of early visual potentials a linear mixed effect model (LMM) was built. As described in section 2.5 the LMM uses a combination of fixed and mixed-effect predictors to form a multiple regression model describing the dependent variable. The dependent variable in this case is the temporal average inside of the segmented EEG. The exported EEG segments were too long to be averaged so the time window for the temporal averaging was selected based on literature and visual inspection of average waveforms over all the data segments.

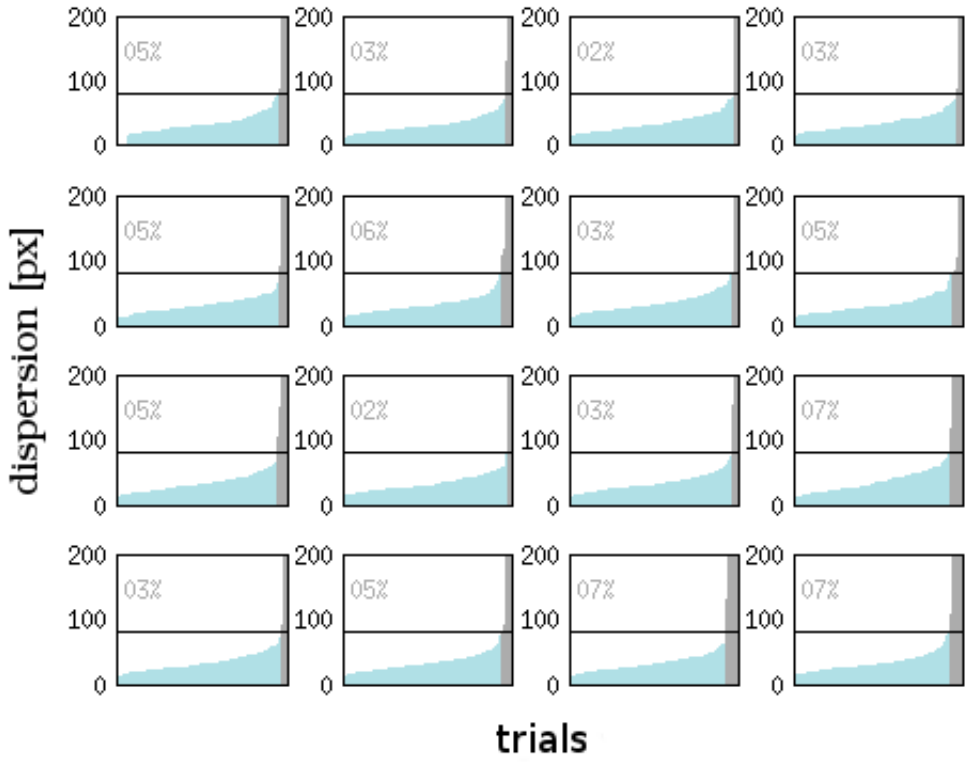

Figure 15: Portions of rejected data marked in grey in 16 grid locations based on fixation dispersion

Purpose of this selection was to assert that the time window contained most of the early visual potential components. There was no averaging over the channels instead the model was constructed separately for each individual channel.

In the LMM model the fixed effects contain the variables of interests. The main goal of the LMM is to find the relationship between the dependent variable and the fixed-effects. Mixed-effects on the other hand are added to the model to explain random variations in the data. In the case of EEG the mixed-effects can also be used to satisfy the assumptions set by the repeated measurements nature of the data. The selection of proper fixed-effects is not a simple task. The process of selecting these effects and the methods used to calculate them are described in section 3.5.2. In turn section 3.5.3 covers the selection of mixed-effects. To improve the accuracy and robustness of the resulting model a model reduction based on the Akaike Information Criterion was performed. Purpose of the reduction was to limit the model to a minimum amount of parameters that best explain the data. Details of the model reduction are in chapter 3.5.5.

3.5.2 Selection of independent fixed-effects

As explained in section 2.4.2 the amplitude of the early visual potentials (especially the P1 potential) is heavily modulated by the parameters of the visual input. These parameters range from relative luminance and contrast to the amount of edges in the perceived area [47][48]. Literature also shows that oculomotor properties of the eye movements (such as the amplitudes of preceding and succeeding saccades) modulate the lambda response of the early visual potentials[76].

As described in section 2.1 the area of acute vision (called fovea in this context) is relatively small. The fovea spans about a 2° patch of the visual field. Using the eye tracker coordinate data it was possible to extract the exact region of the stimulus image which was foveated in each fixation. All of the low-level visual variables were calculated from within this patch. The corresponding fovea size in pixels was calculated separately for each subject using the measured distance between the subject and the monitor. Fovea sizes between subjects had very little variation as the distances to monitor was very homogeneous over the subjects. The low-level visual variables selected for the model were: relative luminance, contrast, kurtosis, skewness, entropy and edge density. Relative luminance is used as an approximation of the luminance experienced by the visual nervous system while inspecting digital images. In gray-scale images the relative luminance corresponds to the pixel intensity values and thus the average of the pixel intensity values inside the fovea patch was used to calculate the RLU variable. Contrast of the patch was calculated in a similar manner as the variance of the pixel intensity values inside the patch. The third and fourth statistical moments (skewness and kurtosis) were also calculated from the pixel intensity values in order to determine the symmetricity and peakedness of the intensity value distribution inside the patch as compared to the normal distribution. Entropy of the patch was also computed as an additional metric for visual saliency [68]. Edge density within the patch was calculated using Sobel approximation. All computed low-level visual fixed-effect variables were z-score standardized by subtracting the mean and dividing by the standard deviation. An example visual input fixed-effect variables sampled from 11 different locations of a randomly selected stimulus picture is displayed in figure 16.

The oculomotor variables used in LMM were calculated using the eye movement events (saccades and fixations) extracted from the recorded eye coordinate data. Because eye movement events were calculated using a high speed algorithm, details regarding the properties of the saccades were already available. Based on earlier research following oculomotor variables were used in the linear mixed effect model: amplitude of the saccade preceding the fixation, amplitude of the saccade succeeding the fixation, fixation duration and total change in gaze direction. The two amplitude variables indicate the distance the eye traveled (in degrees) during the saccade. Fixation duration on the other hand is the total duration of the fixation in milliseconds. The total change in saccade direction was calculated as the angle between the incoming and outgoing saccade. This variable contained only the magnitude of the change (not the direction) and was scaled between 0 to 180 degrees. A total change

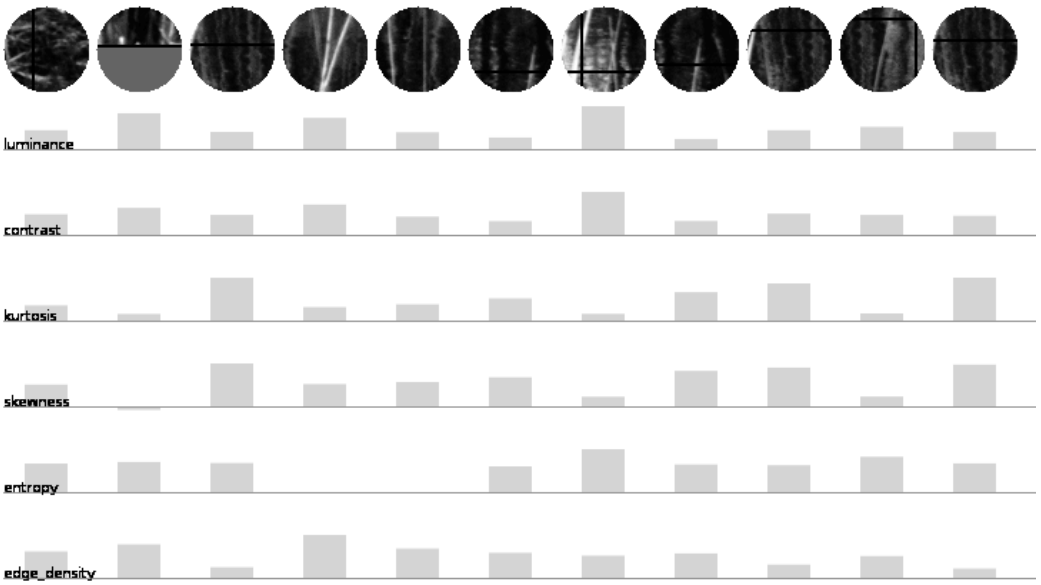

Figure 16: Example of low-level visual input variables

in saccade direction of 0 degrees indicates no change and the succeeding saccade continues in the same direction as the preceding saccades. Conversely a change of 180 degrees corresponds to a complete change in direction and the succeeding saccade travels to the direction of the preceding saccade. As in the case of low-level visual variables the oculomotor variables were also z-score standardized.

Both the low-level visual and oculomotor variables explain the bottom-up processing component of the recorded EEG response. In order to investigate the influence of top-down processing the stimulus condition was also added to the model as a fixed-effect. The stimulus condition was a categorical variable with two states: natural and scrambled. Condition variable was kept out of the model during the initial formulation and model reduction. Once a model describing bottom-up processing had been established the condition variable was added to the model.

3.5.3 Selection of mixed-effects

The mixed-effect variables were added to the model in order to control variations caused by known factors in the data. These variables can be assigned to the model as random intercept or random slopes. For this model all mixed effect were assigned as random intercepts. This decision was based on the fact that literature presented no evidence that mixed effect would have interactions with the amplitude of the early visual potentials. In order to detect which variables should be assigned as mixed effect, variance was calculated with respect to all possible variables not yet assigned as fixed-effect. The sources of variance were calculated from subjects, images, target locations and areas of interest. The results are plotted in figures 17 and 18 as box plots. Inspection of different variances indicated that both subject and image

should be chosen as mixed-effect. This corresponded to theory as EEG recordings can have significant differences between individual subjects. As the stimulus images contained stark local differences the variation caused by different images was not surprising. Location of the target patch within the 4 x 4 grid had no perceivable effect and neither did the image condition (natural vs scrambled). The grid location which the subject was fixating on did not have perceivable differences over the 16 locations.

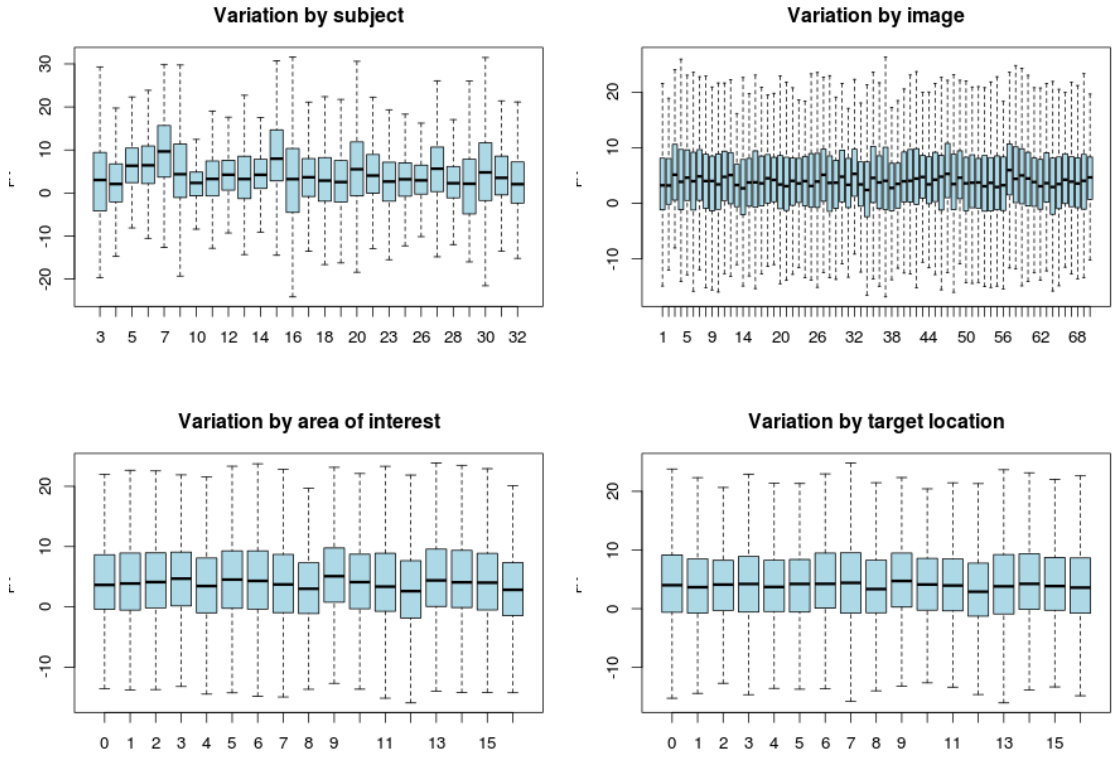

Figure 17: Variance plots

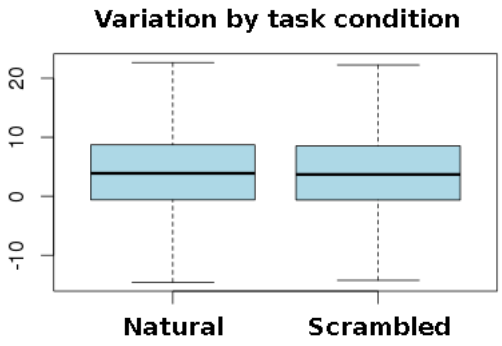

Figure 18: Variance over task condition

In many statistical models the effect of repeated measures must be controlled. Re-

sValue	condIdx	FDU	SDC	PSA	SSA	RLU	CON	KUR	SKE	ENT	EDE
1.51	1	0.000	0.000	0.000	0.000	0.037	0.011	0.016	0.036	0.054	0.022
1.12	1.35	0.000	0.000	0.001	0.001	0.018	0.159	0.215	0.000	0.075	0.069
1.06	1.43	0.325	0.229	0.243	0.000	0.001	0.004	0.007	0.001	0.013	0.048
1.01	1.49	0.001	0.190	0.077	0.658	0.000	0.020	0.002	0.001	0.006	0.001
0.979	1.54	0.223	0.046	0.009	0.011	0.000	0.399	0.043	0.018	0.095	0.011
0.975	1.55	0.243	0.006	0.569	0.008	0.001	0.074	0.016	0.006	0.026	0.038
0.966	1.56	0.045	0.527	0.098	0.320	0.000	0.012	0.010	0.002	0.011	0.020
0.934	1.62	0.153	0.001	0.001	0.002	0.002	0.066	0.045	0.002	0.000	0.754
0.692	2.18	0.007	0.000	0.002	0.000	0.082	0.208	0.267	0.019	0.700	0.003
0.355	4.26	0.002	0.000	0.001	0.000	0.857	0.046	0.379	0.915	0.021	0.035

Table 1: Results of the Belsley Collinearity Diagnostics test

peated measures basically means a situation where multiple samples in the model come from the same source. In this case the problem is very real as the model uses data where there are multiple EEG segments from the same subject. Assigning subject as a mixed effect also solved this problem.

3.5.4 Formulation of the statistical model

First step of formulating the linear mixed effect model was to assert that none of the fixed effect variables were linearly correlated. The absence of collinearity was tested using the Belsley Collinearity Diagnostics test [69]. Results of this test can be found in table 1. All condition indices produced values below 15 indicating that no serious collinearity could be detected.

The resulting linear mixed effect model had a total of 10 fixed effects and 2 mixed effects. Abbreviation used for the variables have been collected in table 2. The resulting equation for the LM-model in R syntax is written in equation 6.

$$\begin{aligned} y \sim RLU + CON + SKE + KUR + ENT + EDE \\ +PSA + SSA + FDU + SDC + (1|SUB) + (1|IMG) \end{aligned} \tag{6}$$

Instead of restricted maximum likelihood (REML) the regular maximum likelihood (ML) was used when calculating the model coefficients. Using ML instead of REML enabled the use of likelihood ratio test when determining the statistical significance of the model.

After the model had been constructed the residual of the model were studied in order to satisfy the other assumptions included in LM-models. Assumptions were tested on EEG channels O1, Oz and O2 as these electrode locations correspond to the visual cortex. As stated in section 2.4.2 this region should provide the best fit for the LM-model as they are closest to the generation site of visually evoked potentials [70] [71]. Figure 19 displays the residuals of the model as a scatter plot for these three electrode locations. From figure 19 it appears that the relationship between

Abbrevation	Variable
Visual	
RLU	Relative luminance
CON	Contrast
KUR	Kurtosis
SKE	Skewness
ENT	Entropy
EDE	Edge density
Oculomotor	
PSA	Preceding saccade amplitude
SSA	Succeeding saccade amplitude
FDU	Fixation duration
SDC	Saccade direction change
Mixed-effects	
SUB	Subject
IMG	Image

Table 2: Variables used in the LMM equation

the visual response and the predicting fixed effect is linear as residuals do not form a curve or other shape that would indicate otherwise. Same figure also indicates that the variance is roughly equal over the fitted values and the fixed-effect can thus be considered homoskedastic. Figure 20 contains the distribution of the residuals as histograms. According to the figure the residuals appear to be normally distributed satisfying the condition of residual gaussianity.

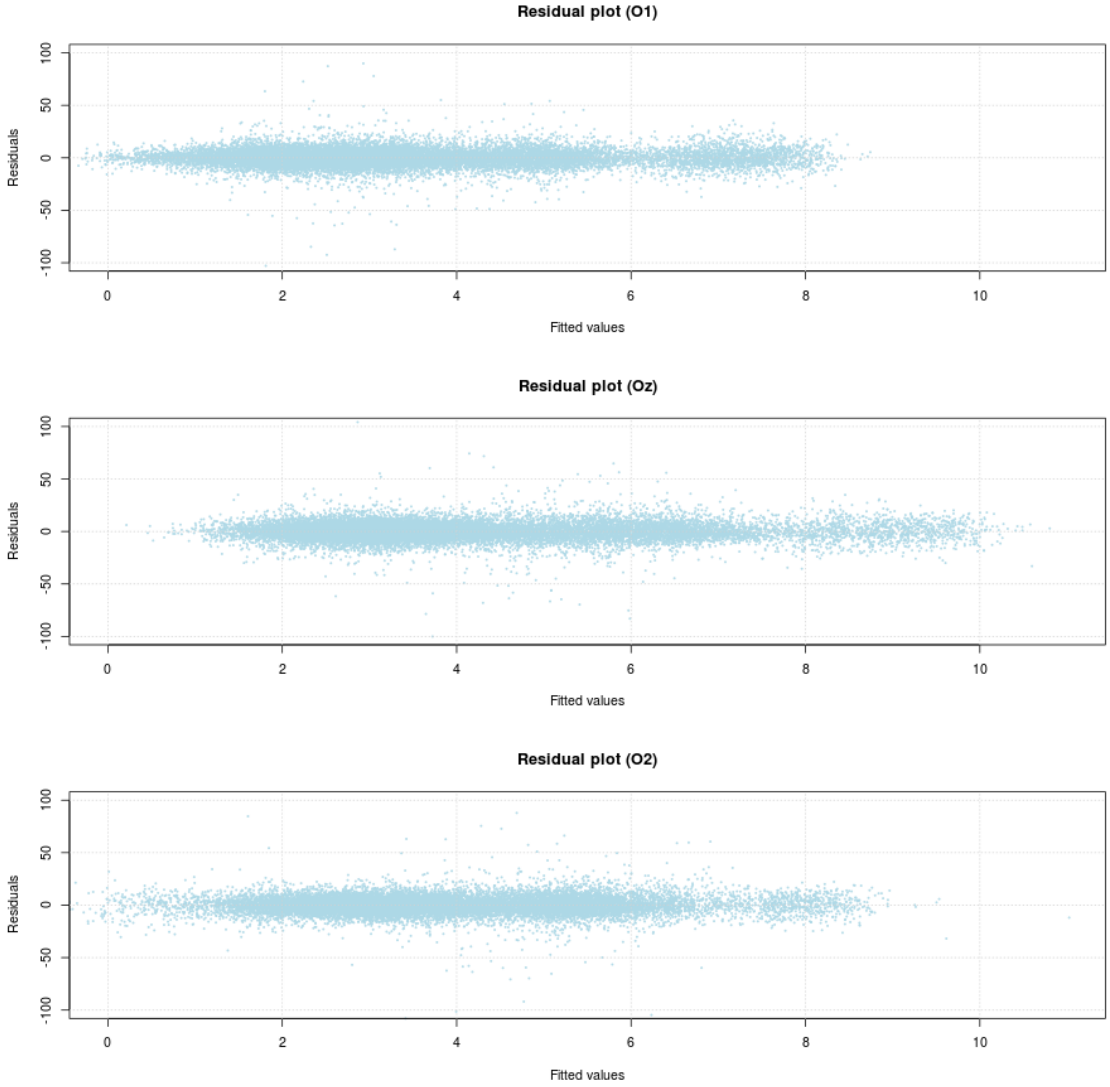

Figure 19: Residual plot of the LM-model in three occipital channels

3.5.5 Reduction of the model

As described in section 2.5, various information criterions (such as the AIC or BIC) can be used to assess how well data fits the assigned model. Using information criterions it is also possible to prune the model down by removing badly fitting variables.

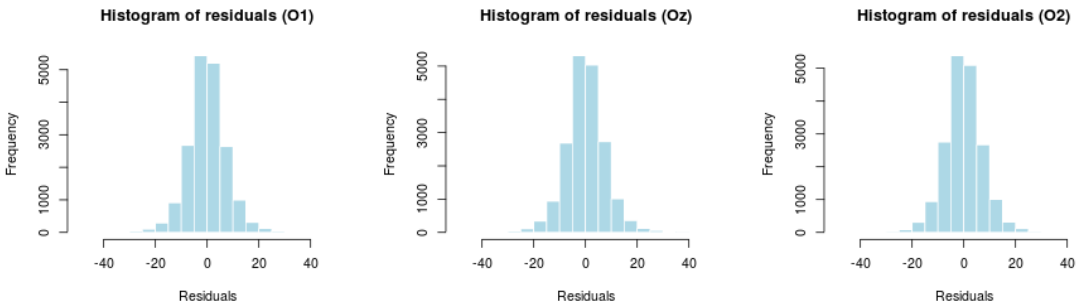

Figure 20: Histograms of residuals in three occipital channels

In this experiment the model reduction was performed using the Akaike Information Criterion. The process was implemented using AIC to conduct a backward selection of features. Reduction was started by first calculating the AIC score for the full model. In the next step AIC score was calculated to models where, in turn, each of the fixed effects were removed. The variable which was responsible for the largest drop in the AIC score was removed from the model and the process was repeated to the new model. This method was iterated until only one variable remained in the model. Again the process was calculated for the three occipital channels and the resulting model reduction curve can be seen in figure 21.

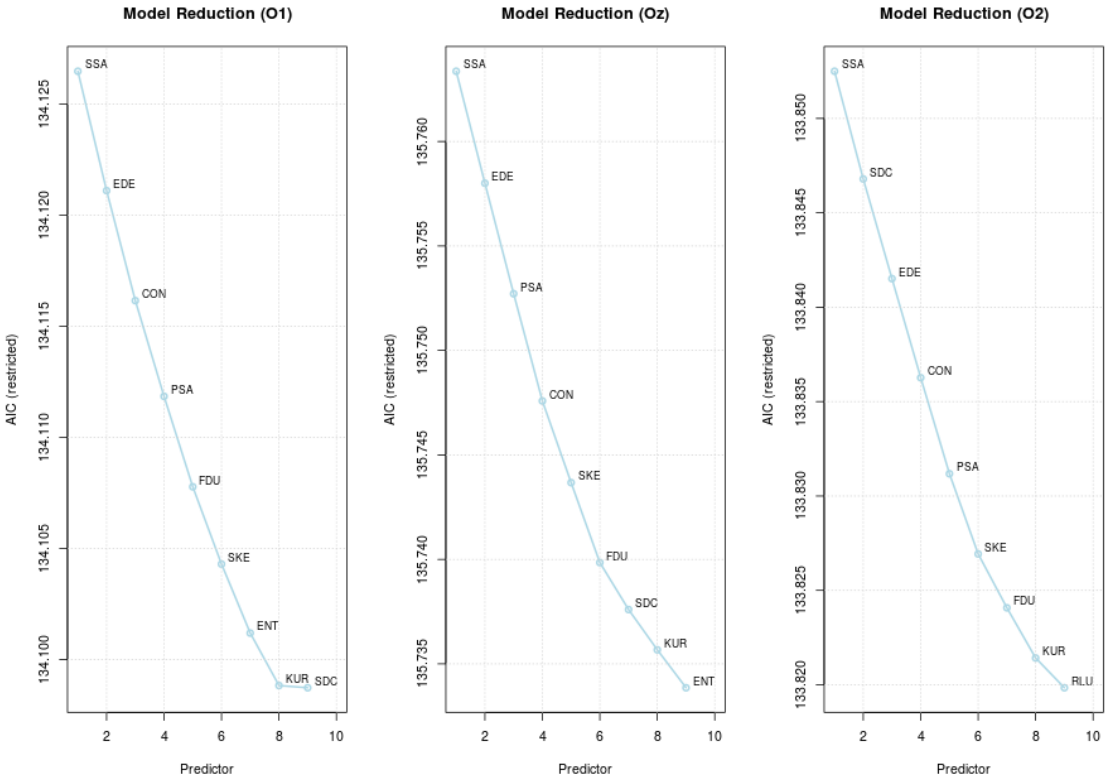

Figure 21: AIC-based stepwise model reduction for channels O1, Oz and O2

From the results it seemed plausible that oculomotor variables and the low-level visual variables should be separated into individual models. According to the model reduction oculomotor and visual variables were analysed as separate models. Furthermore, the edge density variable (EDE) was removed from the visual model as it received poor scoring in all three electrode locations. The resulting LMM equations in R syntax are in equations 7 and 8.

$$y \sim RLU + CON + SKE + KUR + ENT + (1|SUB) + (1|IMG) \tag{7}$$

$$y \sim FDU + PSA + SSA + SDC + (1|SUB) + (1|IMG) \tag{8}$$

3.5.6 Statistical significance testing

To quantify the reliability of the generated model a likelihood-ratio test (LRT) was used. Testing was implemented as a two-step process and performed on both of the models formed on the basis of the model reduction. In the first step the model of each channel was compared to a model consisting only of the mixed-effects. The reduced model is referred to as *null model* in this context. The three hypothesis to be tested were labeled H0 (null model) H1.1 (visual input model) and H1.2 (oculomotor model). In the second step another, within-model LRT, was computed for electrode locations which were found significant in the first step. In this second test the significances of the different fixed-effect variables inside the model were computed. LRT is described in section 2.5 and the testing was performed using the R lmerTest library [72]. The tested hypotheses are listed below.

- H0: Low-level visual and oculomotor variables do not modulate the amplitude of early visual potentials
- H1.1: Low-level visual variables modulate the amplitude of early visual potentials
- H1.2: Oculomotor variables modulate the amplitude of early visual potentials

The effect of top-down processing was investigated by adding the stimulus condition in both of the models as a fixed-effect variable. The effect of stimulus condition was then tested by comparing these models to visual input and oculomotor models. The new models containing the top-down component were labeled as H2.1 (for the visual input model) and H2.2 (for the oculomotor model).

- H2.1: Low-level visual variables and the stimulus condition modulate the amplitude of early visual potentials
- H2.2: Oculomotor variables and the stimulus condition modulate the amplitude of early visual potentials

4 Results

The LMM analysis produced two separate models explaining the generation of the early visual potential. First model explained the amplitude of the response in terms of visual input and the second model in terms of oculomotor variables. With each model the top-down effect of stimulus condition (natural vs scrambled) was also investigated as an additional likelihood ratio test.

The statistical significance of the visual model in all of the electrode locations is presented in figure 22. Statistical significances were obtained by comparing the null model and the actual model using LRT. Most of the significant electrode locations were near the occipital lobe with few exceptions in the right tempo-frontal region. These exceptions do not fit the theory and considering their location are most likely caused by some residual eye movement artifacts in the data. It is also possible that the result was caused by minor heteroscedasticity of the data which can produce false positives in linear regression models [73]. Further analysis of the statistically significant tempo-frontal electrode group was thus omitted.

Model coefficients for the six strongly significant ($p<0.01$) channels around the occipital and parietal lobes are plotted in figure 23. These electrode locations correspond to the visual cortex where the effect should be predominant due to the suitable alignment of the signal sources. Results of the within-model LRT are also color-coded into the figure indicating strong and very strong presumptions against the null hypothesis. The exact values for the visual input model can also be found in appendix A.

In the visual input model fixed-effect coefficients for the relative luminance and kurtosis had a positive correlation with the dependent variable. In other words, the model indicates that an increase in either of these values will result in a larger amplitude for the early visual potential response. Out of the two, the effect of relative luminance was larger and more consistent over the locations. Skewness of the fovea patch had a positive correlation with the early visual potential amplitude in all locations except PO8 where the coefficient was slightly negative. The entropy fixed-effect coefficient was negative in all of the channel locations. The fixed-effect for contrast had positive correlation in both left and right sides of the occipital and parieto-occipital electrode sites. In the occipital midline (Oz and Iz), however, the coefficient was negative. The results of the within-model LRT test over the channels of the left hemisphere (locations O1 and PO7) indicated that both relative luminance and kurtosis had strong statistical significance. On the right hemisphere (O2 and PO8) only entropy had strong significance. On the midline both relative luminance and entropy were statistically significant. In the light of these results the H0 hypothesis for the visual model could be discarded. The early visual potential is clearly modulated by low-level visual features so the alternative hypothesis H1.1 could be accepted. The resulting model describes how various low-level visual features of the observed region in a natural stimuli contribute to the generation of the early visual response.

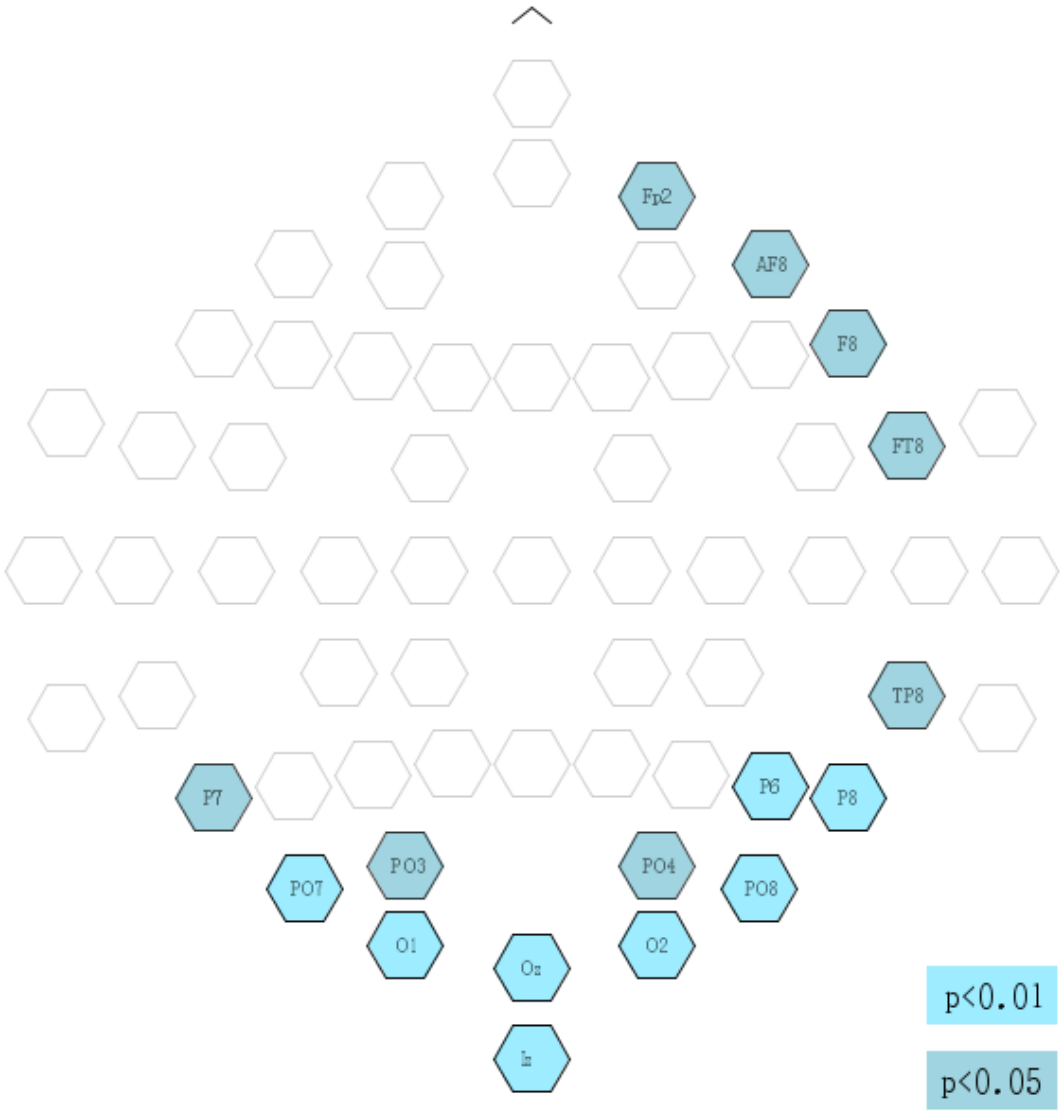

Figure 22: Results of LRT for visual input model

Second model explained the response amplitude as a combination of oculomotor variables. Results of the LRT comparing null model to the oculomotor model are in figure 24.

Model coefficients of six of the most strongly significant channels are plotted in figure 25. As with the visual input model the strong and very strong significances are indicated with different colors. The exact values for the oculomotor model can also be found in appendix B.

In the oculomotor models of the six electrode locations succeeding saccade amplitude, saccade direction change and fixation duration had negative correlation to early visual potential amplitude. Conversely the amplitude of the preceding saccade had a positive correlation. In all 6 electrode sites saccade direction change and

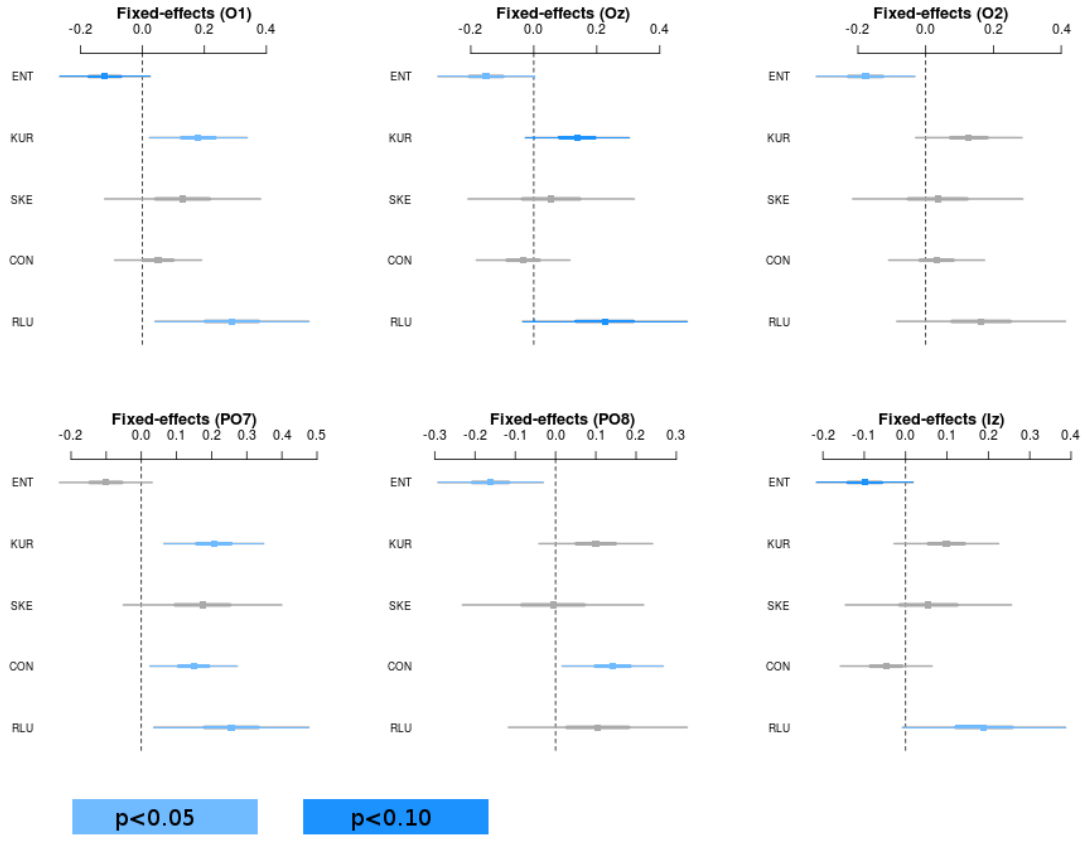

Figure 23: Model coefficients for visual input model

preceding saccade amplitude fixed effects were statistically significant according the the within-model LRT.

The effect of stimulus condition on the amplitude of the early visual potential was examined by inserting stimulus condition as a fixed-effect variable into both models. Using the same six channels for visual input and oculomotor models yielded no statistically significant results in the test. It would appear that stimulus condition does not modulate the amplitude and hypotheses H2.1 and H2.2 regarding the top-down effect could be discarded.

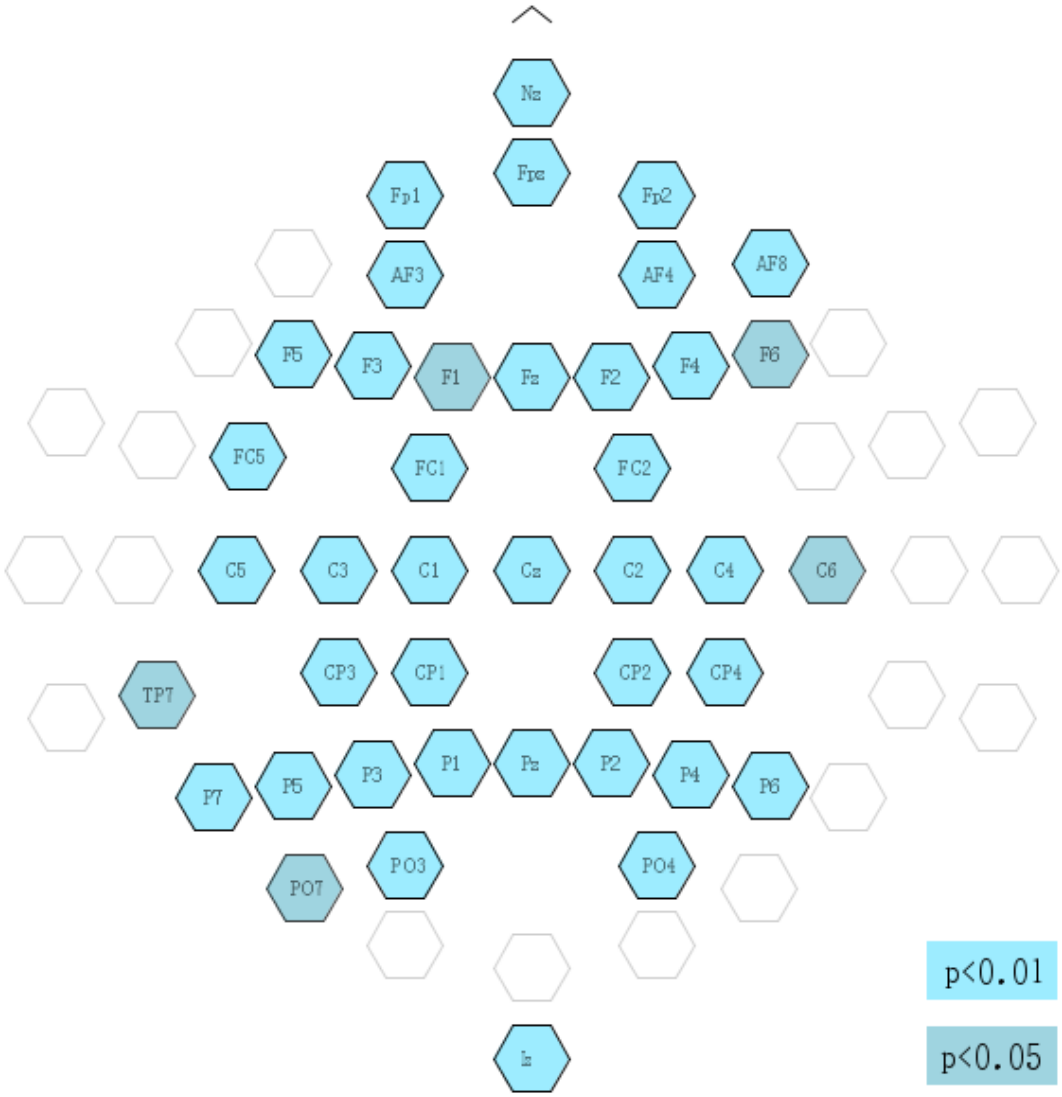

Figure 24: Results of LRT for oculomotor model

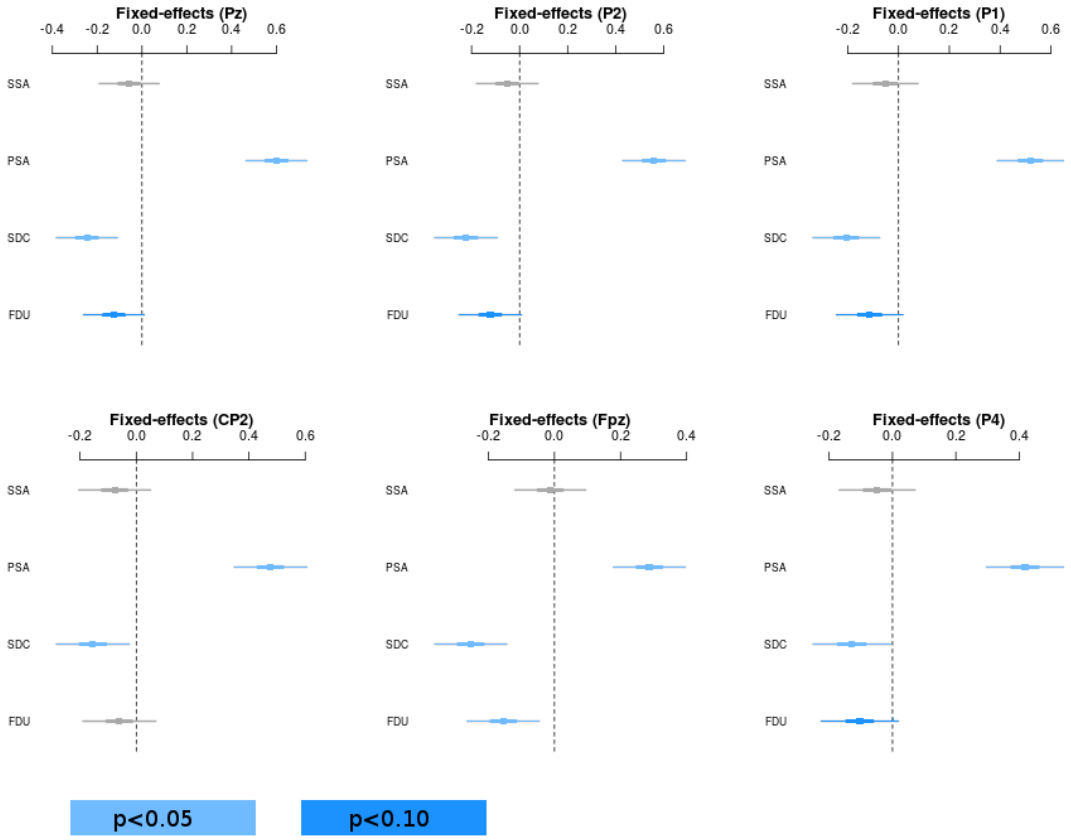

Figure 25: Model coefficients for oculomotor model

5 Summary and discussion

5.1 Evaluation of the experimental design and implementation

The experimental design and implementation of the experiment worked well. During the recording and analysis stage there were no unexpected factors which would have hindered the reliability of the results. The only problem with the setup was the long duration of each recording session, therefore, most subjects were visibly fatigued after the experiment. The long duration resulted from the need to obtain multiple repetitions for statistically reliable analysis of the collected data. Furthermore, setting up the recording apparatus and preparing the subject took a considerable amount of time. In this experiment the effect of fatigue, however, was controlled by dividing the experiment into five blocks of equal length and reversing presentation order of the blocks for half of the subjects. With this counterbalancing the effect of fatigue should not have affected the analysis.

Implementation of multiple registration methods in the experiment was successful. Temporal synchronicity between the two recording methodologies was achieved through external triggering of the two data streams by a computer controlling the displaying of stimulus images. Analysis methods enabled the extraction of EEG data segments synchronized to the fixation onsets of the eye tracking coordinate data. The implemented eye tracker calibration quality validation test could be used to quantify the calibration accuracy and precision in various locations of the calibration area. Results of this validation test could then be utilized to remove data with poor accuracy regarding eye movements thus improving the reliability of the statistical analysis. This method also enabled the selective removal of partially corrupted eye movement data, thus saving more data for later processing steps than traditional rejection methods.

5.2 Evaluation of results

In the statistical analysis a linear mixed-effect model was generated to explain the recorded early visual potential amplitude of the processed EEG segments as a function of low-level visual and oculomotor parameters. According to AIC-based model reduction analysis a single model could not sufficiently explain both visual and oculomotor variables so the model was split into two separate models. Contrary to existing theory the model reduction analysis suggests that the interaction between visual input and oculomotor variables was minimal on the occipital electrode site. This observation seems plausible when comparing the regions of statistical significance in both models. In both models the subject and the observed stimulus image were assigned as mixed-effect variables. Both models were tested against a null model hypothesis using the LRT method in order to determine electrode sites where the model was statistically significant. In addition another within-model LRT was

computed for the six most significant electrode locations in both model types to discover the statistically significant coefficients.

5.2.1 Visual model

The visual input model was significant in all of the occipital electrode sites which coincided with the existing theoretical framework. The model, however, was also significant in tempo-frontal electrode sites which could not be explained by earlier research. The tempo-frontal electrodes were thus assumed to be caused by residual artifacts or heteroscedasticity in the data.

In the six channel locations closest to the visual cortex the relative luminance was found to have positive correlation with the response amplitude. This finding coincides with earlier literature [47] which also reports a positive modulation of the P1 response by stimulus luminance. Earlier research [74] also reports that contrast has been found to correlate positively with the amplitude of the early visual responses. The positive modulation of contrast was observed in four of the six electrode locations where only the midline electrodes (Oz and Iz) had an opposite effect.

The effect of kurtosis and skewness of the perceived stimuli on the early visual response has not been researched in the past. According to results found in this experiment the skewness produced no statistically significant modulations on any of the six locations. Likewise kurtosis was found to be significant in only two of the locations. It is thus plausible that third and fourth statistical central moments do not have significant contributions to the generation of the early visual potential.

No earlier ERP research has focused on the effect of local entropy in naturalistic stimuli but earlier eye-tracking study [75] suggests that entropy plays a role in bottom-up visual attention. In this experiment the entropy of the visual input had a negative correlation in all of the electrode sites and was statistically significant in five sites. This result is perplexing as both contrast and entropy describe the complexity of the image but their correlations in the LM-model are opposite.

5.2.2 Oculomotor model

The oculomotor model produced conflicting results. The model was significant in a much larger quantity of channels. The most significant electrode cluster was focused around the central and parietal regions of the scalp. Examining the coefficients for the oculomotor model it appeared that the largest overall contribution to the response amplitude was caused by the amplitude of the preceding saccade (PSA). The PSA fixed-effect variable is significant in all of the six locations and has the largest magnitude of all the model coefficients.

The two primary signal generators for saccade related potentials are the lambda response and the saccadic spike potential. Lambda response originates from the

posterior-parietal region where as saccadic spike potential is localized around the frontal eye-fields and radiates towards the parietal and central regions. According to the electrode locations of the model it would appear that the model is more dependent on the saccadic spike potential. The SP, however, peaks around the saccade onset where as the analyzed time-window starts 50 ms after the fixation onset. Purely based on the temporal characteristics it is more plausible that the origin of the response would be the lambda response.

Taking into account the relatively large spread of the statistically significant electrodes and the centralized location of the strongest result it is obvious the model does not fit the data perfectly. Most likely the oculomotor model does model the underlying saccade related potentials but is either lacking fixed-effects or the dependent variable is selected poorly. It is plausible that the selected time window does not fully capture the saccade related potential. The model could theoretically be improved by using localized sources as the dependent variable instead of the electrodes. Tuning of the model through source localization is briefly discussed in section 6 while mapping the possible avenues of future research. It would also be desirable to attempt integration with the visual model as particularly the lambda response has been shown to interact with the parameters of the visual input [76].

5.2.3 Top-down vs. bottom-up processing

In this experiment the data indicated no evidence that early processing of the stimuli on the visual cortex would be affected by top-down processing. The presented results are compatible with the theory that early time-windows are primarily affected by visual and oculomotor features. Majority of the earlier research also reports top-down modulation only in later ERP components [77] [78]. The observed results should not, however, be interpreted as solid evidence for the absence of top-down influence to early visually evoked potentials. The effect of top-down processing in early visual attention has been reported in the past [79] [80] [81].

5.3 Global normalization

Results of this experiment indicate that even though all of the stimulus images were globally normalized, large local differences still exist within each image. In other words: the low-level visual input in fovea sized patches is different depending on which region of the image the subject was fixating in. Due to these local differences the amplitudes of early visual EEG responses (C1, P1, lambda) differ between various regions of the stimulus. In the light of these results its reasonable to claim that global normalization is not an acceptable normalization method to control stimuli when investigating visual responses with EEG or MEG. The amplitude modulation caused by local variation inside the stimulus image must be accounted for by some other method. One possible method is to model the effect of the visual input using a LMM-based modeling approach. Analysis of EEG should also move away from

using large group averages [82] and focus more on the single-trial level of the data. This shift has already begun and there are tools to support this approach [83].

6 Future research

During the experiment a large amount of physiological data was collected using three different registration methodologies. This thesis covers the collection of all of the datasets but only the analysis of eye movement and EEG recordings. The entire data set could be used to further refine the current analysis method or it can be used to develop entirely new analysis protocols. This section aims to map out the possible courses for future research within the boundaries of this experiment. Application of the experimental paradigm to other recording methodologies is also briefly discussed.

From all the collected neural data only EEG was analyzed with the linear mixed model. The accuracy of the current method can be increased by first performing a *source localization* for the recorded EEG data and then substituting those sources into the LM model as dependent variables. In source localization a mathematical model is used to estimate the current density responsible for the recorded potential on the scalp. The difficulty of estimating neural signal generators is more commonly known as the inverse problem. This approach can be further improve by using MEG data along with the EEG data for source localization. Due to the higher sensitivity towards deep sources and the higher amount of sensors in the MEG recording, the collected data can be used to complement the EEG recording when performing source localization. With proper localization the model gains more robustness and accuracy as it then models the estimated physiological signal generator and not just the recorded potentials from the scalp. Source localization is not a trivial procedure and one of the problems that must be solved is the selection of the source modeling method. The two classes of source models are the dipole model and the source distribution model. Out of these two classes the dipole model is parametric and the distributed sources a non-parametric method for localization. Source localization could be improved as well by acquiring anatomical MR images for each subject. With anatomical MR images the spatial alignment of sources can be calculated more accurately for each subject than when using an average template [84].

In the current statistical analysis only one dependent variable was used. This variable was the temporal average of each processed EEG segment from 50 to 100 ms after the fixation-onset. In the future research it would be interesting to break this time-window into multiple dependent variables in and investigate the effects on low-level variables and top-down factors in different overlapping latencies. This approach seems logical as the current dependent variable is known to contain partially overlapping components from at least three different responses (C1, P1 and lambda). Performing the analysis again with a combination of different time windows could yield more information about the relationship between low-level variables and the response amplitude.

Another interesting topic of future research is the use of the same experimental design with another recording methodology. It might be beneficial to run the same experiment using a functional magnetic resonance imaging (fMRI) for data acqui-

sition. fMRI is a brain imaging technique which is based on recording the flow of oxygenated blood (known as BOLD response) to various parts of the brain and the central nervous system. The increased in load in certain parts of the brain (like the occipital lobe in case of visual stimulus) can be detected as an increase of blood flow into that region. Thus fMRI enables an indirect way of measuring brain activity as a physiological response rather than an electric one. With some fMRI devices it is also possible to record EEG concurrently with the fMRI [85] which would produce synchronized data from both the hemodynamic response and the electrical activity of the brain.

References

[1] World Medical Association. (2000). Declaration of Helsinki, ethical principles for medical research involving human subjects. 52 nd WMA General Assembly, Edinburgh, Scotland.

[2] Dimigen, O., Sommer, W., Hohlfeld, A., Jacobs, A. M., and Kliegl, R. (2011). Coregistration of eye movements and EEG in natural reading: analyses and review. Journal of Experimental Psychology: General, 140(4), 552.

[3] Connor, C. E., Egeth, H. E., and Yantis, S. (2004). Visual attention: bottom-up versus top-down. Current Biology, 14(19), R850-R852.

[4] Le Meur, O., Le Callet, P., Barba, D., & Thoreau, D. (2006). A coherent computational approach to model bottom-up visual attention. Pattern Analysis and Machine Intelligence, IEEE Transactions on, 28(5), 802-817.

[5] Hopfinger, J. B., Buonocore, M. H., & Mangun, G. R. (2000). The neural mechanisms of top-down attentional control. Nature neuroscience, 3(3), 284-291.

[6] Itti, Laurent. Models of bottom-up and top-down visual attention. Diss. California Institute of Technology, 2000.

[7] Robinson, D. A. (1964). The mechanics of human saccadic eye movement. The Journal of physiology, 174(2), 245-264.

[8] Matin, E. (1974). Saccadic suppression: a review and an analysis. Psychological bulletin, 81(12), 899.

[9] Liversedge, S. P., & Findlay, J. M. (2000). Saccadic eye movements and cognition. Trends in cognitive sciences, 4(1), 6-14.

[10] Martinez-Conde, S., Macknik, S. L., Troncoso, X. G., and Dyar, T. A. (2006). Microsaccades counteract visual fading during fixation. Neuron, 49(2), 297-305.

[11] Robinson, D. A. (1965). The mechanics of human smooth pursuit eye movement. The Journal of Physiology, 180(3), 569.

[12] Malmivuo, J., and Plonsey, R. (1995). Bioelectromagnetism: principles and applications of bioelectric and biomagnetic fields. Oxford University Press.

[13] Malmivuo, J., & Plonsey, R. (1995). Bioelectromagnetism: principles and applications of bioelectric and biomagnetic fields. Retrieved 4.9.2014 from http://www.bem.fi/book/28/fi/2801.gif

[14] Fang, F., & He, S. (2005). Cortical responses to invisible objects in the human dorsal and ventral pathways. Nature neuroscience, 8(10), 1380-1385.

[15] Van Der Velde, F., & De Kamps, M. (2001). From knowing what to knowing where: Modeling object-based attention with feedback disinhibition of activation. Journal of Cognitive Neuroscience, 13(4), 479-491.

[16] DuBois, R. M., and Cohen, M. S. (2000). Spatiotopic organization in human superior colliculus observed with fMRI. Neuroimage, 12(1), 63-70.

[17] Malmivuo, J., & Plonsey, R. (1995). Bioelectromagnetism: principles and applications of bioelectric and biomagnetic fields. Retrieved 4.9.2014 from http://www.bem.fi/book/28/fi/2802.gif

[18] Willenbockel, V., Sadr, J., Fiset, D., Horne, G. O., Gosselin, F., and Tanaka, J. W. (2010). Controlling low-level image properties: the SHINE toolbox. Behavior research methods, 42(3), 671-684.

[19] Knebel, J. F., Toepel, U., Hudry, J., le Coutre, J., & Murray, M. M. (2008). Generating controlled image sets in cognitive neuroscience research. Brain topography, 20(4), 284-289.

[20] Greenwald, A. G. (1976). Within-subjects designs: To use or not to use?. Psychological Bulletin, 83(2), 314.

[21] Macfie, H. J., Bratchell, N., Greenhoff, K., & Vallis, L. V. (1989). Designs to balance the effect of order of presentation and first-order carry-over effects in hall tests. Journal of Sensory Studies, 4(2), 129-148.

[22] Henson, R. (2007). Efficient experimental design for fMRI. Statistical parametric mapping: The analysis of functional brain images, 193-210.

[23] Box, G. E., Hunter, W. G., & Hunter, J. S. (1978). Statistics for experimenters.

[24] Peirce, J. W. (2007). PsychoPy?psychophysics software in Python. Journal of neuroscience methods, 162(1), 8-13.

[25] Jacob, R. J., and Karn, K. S. (2003). Eye tracking in human-computer interaction and usability research: Ready to deliver the promises. Mind, 2(3), 4.

[26] Pieters, R. (2008). A review of eye-tracking research in marketing. Review of marketing research, 4, 123-147.

[27] Rayner, K. (1998). Eye movements in reading and information processing: 20 years of research. Psychological bulletin, 124(3), 372.

[28] Henderson, J. M., and Pierce, G. L. (2008). Eye movements during scene viewing: Evidence for mixed control of fixation durations. Psychonomic Bulletin & Review, 15(3), 566-573.

[29] Young, L. R., and Sheena, D. (1975). Eye-movement measurement techniques. American Psychologist, 30(3), 315.

[30] Kaufman, A. E., Bandopadhay, A., and Shaviv, B. D. (1993, October). An eye tracking computer user interface. In Virtual Reality, 1993. Proceedings., IEEE 1993 Symposium on Research Frontiers in (pp. 120-121). IEEE.

[31] Robinson, D. A. (1963). A method of measuring eye movemnent using a scieral search coil in a magnetic field. Bio-medical Electronics, IEEE Transactions on, 10(4), 137-145.

[32] Hess, C. W., Muri, R., and Meienberg, O. (1986). Recording of horizontal saccadic eye movements: Methodological comparison between electro-oculography and infrared reflection oculography. Neuro-ophthalmology, 6(3), 189-197.

[33] Sewell, W., and Komogortsev, O. (2010, April). Real-time eye gaze tracking with an unmodified commodity webcam employing a neural network. In CHI'10 Extended Abstracts on Human Factors in Computing Systems (pp. 3739-3744). ACM.

[34] Salvucci, D. D., and Goldberg, J. H. (2000, November). Identifying fixations and saccades in eye-tracking protocols. In Proceedings of the 2000 symposium on Eye tracking research and applications (pp. 71-78). ACM.

[35] Nyström, M., & Holmqvist, K. (2010). An adaptive algorithm for fixation, saccade, and glissade detection in eyetracking data. Behavior research methods, 42(1), 188-204.

[36] Yoshinaga, H., Nakahori, T., Ohtsuka, Y., Oka, E., Kitamura, Y., Kiriyama, H., ... and Hoshida, T. (2002). Benefit of simultaneous recording of EEG and MEG in dipole localization. Epilepsia, 43(8), 924-928.

[37] The Elekta Neuromag Vectorview System (2013, August), Retrieved 10.9.2014 from http://imaging.mrc-cbu.cam.ac.uk/meg/VectorviewDescription

[38] Croft, R. J., and Barry, R. J. (2000). Removal of ocular artifact from the EEG: a review. Neurophysiologie Clinique/Clinical Neurophysiology, 30(1), 5-19.

[39] Fatourechi, M., Bashashati, A., Ward, R. K., and Birch, G. E. (2007). EMG and EOG artifacts in brain computer interface systems: A survey. Clinical neurophysiology, 118(3), 480-494.

[40] Kamienkowski, J. E., Ison, M. J., Quiroga, R. Q., and Sigman, M. (2012). Fixation-related potentials in visual search: a combined EEG and eye tracking study. Journal of vision, 12(7), 4.

[41] Mehani, O., Taib, R., & Itzstein, B. (2014, September). Time calibration in experiments with networked sensors. In Local Computer Networks (LCN), 2014 IEEE 39th Conference on (pp. 386-389). IEEE.

[42] Sebel, P. S., Lang, E., Rampil, I. J., White, P. F., Cork, R., Jopling, M., ... and Manberg, P. (1997). A multicenter study of bispectral electroencephalogram analysis for monitoring anesthetic effect. Anesthesia and Analgesia, 84(4), 891-899.

[43] Kok, A. (1997). Event-related-potential (ERP) reflections of mental resources: a review and synthesis. Biological psychology, 45(1), 19-56.

[44] Luck, S. J. (2014). An introduction to the event-related potential technique. MIT press

[45] Khoshbin, S., and Hallett, M. (1981). Multimodality evoked potentials and blink reflex in multiple sclerosis. Neurology, 31(2), 138-138.

[46] Taylor, M. J. (2002). Non-spatial attentional effects on P1. Clinical Neurophysiology, 113(12), 1903-1908.

[47] Johannes, S., Münte, T. F., Heinze, H. J., and Mangun, G. R. (1995). Luminance and spatial attention effects on early visual processing. Cognitive Brain Research, 2(3), 189-205.

[48] Hansen, B. C., Johnson, A. P., and Ellemberg, D. (2011). Natural Scene Image Complexity Differentially Modulates the N1 and P1 Components of Early VEPs. Journal of Vision, 11(11), 1121-1121.

[49] Everling, S., Krappmann, P., & Flohr, H. (1997). Cortical potentials preceding pro-and antisaccades in man. Electroencephalography and clinical neurophysiology, 102(4), 356-362.

[50] Jagla, F., Jergelova, M., & Riecansky, I. (2007). Saccadic eye movement related potentials. Physiological research, 56(6), 707.

[51] Kazai, K., & Yagi, A. (2005, March). Contrast dependence of lambda response. In International Congress Series (Vol. 1278, pp. 61-64). Elsevier.

[52] Thickbroom, G. W., & Mastaglia, F. L. (1985). Presaccadic ?spike?potential: investigation of topography and source. Brain research, 339(2), 271-280.

[53] Carl, C., Açk, A., König, P., Engel, A. K., & Hipp, J. F. (2012). The saccadic spike artifact in MEG. Neuroimage, 59(2), 1657-1667.

[54] Moster, M. L., & Goldberg, G. (1990). Topography of scalp potentials preceding self initiated saccades. Neurology, 40(4), 644-644.

[55] Corbeil, R. R., and Searle, S. R. (1976). Restricted maximum likelihood (REML) estimation of variance components in the mixed model. Technometrics, 18(1), 31-38.

[56] Santos Nobre, J., & da Motta Singer, J. (2007). Residual analysis for linear mixed models. Biometrical Journal, 49(6), 863-875.

[57] Winter, B. (2013). Linear models and linear mixed effects models in R with linguistic applications. arXiv:1308.5499.

[58] Akaike, H. (1976). An information criterion (AIC). Math Sci, 14(153), 5-9

[59] Bozdogan, H. (1987). Model selection and Akaike's information criterion (AIC): The general theory and its analytical extensions. Psychometrika, 52(3), 345-370.

[60] Van Der Linde, I., Rajashekar, U., Bovik, A. C., and Cormack, L. K. (2009). DOVES: a database of visual eye movements. Spatial vision, 22(2), 161-177.

[61] Avanaki, A. N. (2009). Exact global histogram specification optimized for structural similarity. Optical review, 16(6), 613-621.

[62] Foulsham, T., Alan, R., and Kingstone, A. (2011). Scrambled eyes? Disrupting scene structure impedes focal processing and increases bottom-up guidance. Attention, Perception, and Psychophysics, 73(7), 2008-2025.

[63] Taulu, S., Simola, J., and Kajola, M. (2005). Applications of the signal space separation method. Signal Processing, IEEE Transactions on, 53(9), 3359-3372.

[64] Ille, N., Berg, P., and Scherg, M. (2002). Artifact correction of the ongoing EEG using spatial filters based on artifact and brain signal topographies. Journal of clinical neurophysiology, 19(2), 113-124.

[65] Smeets, J. B., and Hooge, I. T. (2003). Nature of variability in saccades. Journal of neurophysiology, 90(1), 12-20.

[66] Team, R. C. (2012). R: A language and environment for statistical computing.

[67] Bates, D., Maechler, M., and Bolker, B. (2012). lme4: Linear mixed-effects models using S4 classes.

[68] Li, Y., Zhou, Y., Yan, J., Niu, Z., and Yang, J. (2010). Visual saliency based on conditional entropy. In Computer Vision?ACCV 2009 (pp. 246-257). Springer Berlin Heidelberg.

[69] Belsley, D. A., Kuh, E., and Welsch, R. E. (2005). Regression diagnostics: Identifying influential data and sources of collinearity (Vol. 571). John Wiley and Sons.

[70] Makeig, S., Westerfield, M., Jung, T. P., Enghoff, S., Townsend, J., Courchesne, E., and Sejnowski, T. J. (2002). Dynamic brain sources of visual evoked responses. Science, 295(5555), 690-694.

[71] Gonzalez, C. M. G., Clark, V. P., Fan, S., Luck, S. J., and Hillyard, S. A. (1994). Sources of attention-sensitive visual event-related potentials. Brain topography, 7(1), 41-51.

[72] Kuznetsova, A., Brockhoff, P. B., and Christensen, R. H. B. (2013). lmerTest: Tests for random and fixed effects for linear mixed effect models (lmer objects of lme4 package). R package version, 2-0.

[73] Long, J. S., & Ervin, L. H. (2000). Using heteroscedasticity consistent standard errors in the linear regression model. The American Statistician, 54(3), 217-224.

[74] Macé, M. J. M., Thorpe, S. J., and Fabre?Thorpe, M. (2005). Rapid categorization of achromatic natural scenes: how robust at very low contrasts?. European Journal of Neuroscience, 21(7), 2007-2018.

[75] Reinagel, P., and Zador, A. M. (1999). Natural scene statistics at the centre of gaze. Network: Computation in Neural Systems, 10(4), 341-350.

[76] Gaarder, K., Krauskopf, J., Graf, V., Kropfl, W., and Armington, J. C. (1964). Averaged brain activity following saccadic eye movement. Science, 146(3650), 1481-1483

[77] Ansorge, U., Kiss, M., Worschech, F., & Eimer, M. (2011). The initial stage of visual selection is controlled by top-down task set: new ERP evidence. Attention, Perception, & Psychophysics, 73(1), 113-122.

[78] Shigeto, H., Ishiguro, J., & Nittono, H. (2011). Effects of visual stimulus complexity on event-related brain potentials and viewing duration in a free-viewing task. Neuroscience letters, 497(2), 85-89.

[79] Gazzaley, A., Cooney, J., McEvoy, K., Knight, R., and D'esposito, M. (2005). Top-down enhancement and suppression of the magnitude and speed of neural activity. Cognitive Neuroscience, Journal of, 17(3), 507-517.

[80] Rauss, K., Schwartz, S., & Pourtois, G. (2011). Top-down effects on early visual processing in humans: a predictive coding framework. Neuroscience & Biobehavioral Reviews, 35(5), 1237-1253.

[81] Kirchner, H., & Thorpe, S. J. (2006). Ultra-rapid object detection with saccadic eye movements: Visual processing speed revisited. Vision research, 46(11), 1762-1776.

[82] Rousselet, G. A., and Pernet, C. R. (2011). Quantifying the time course of visual object processing using ERPs: it's time to up the game. Frontiers in psychology, 2.

[83] Pernet, C. R., Chauveau, N., Gaspar, C., and Rousselet, G. A. (2011). LIMO EEG: a toolbox for hierarchical LInear MOdeling of ElectroEncephaloGraphic data. Computational intelligence and neuroscience, 2011, 3.

[84] Dale, A. M., and Sereno, M. I. (1993). Improved localizadon of cortical activity by combining eeg and meg with mri cortical surface reconstruction: A linear approach. Journal of cognitive neuroscience, 5(2), 162-176.

[85] Mulert, C., Jäger, L., Schmitt, R., Bussfeld, P., Pogarell, O., Möller, H. J., ... and Hegerl, U. (2004). Integration of fMRI and simultaneous EEG: towards a comprehensive understanding of localization and time-course of brain activity in target detection. Neuroimage, 22(1), 83-94.

A Visual model coefficients

		Estimate	Std. Error	df	t value	Pr(>|t|)
Iz	(Intercept)	2.71	0.30	27.12	9.03	0.00
	RLU	0.19	0.10	2439.00	1.89	0.06
	CON	-0.05	0.06	1202.11	-0.83	0.41
	SKE	0.06	0.10	6625.49	0.54	0.59
	KUR	0.10	0.06	12743.52	1.53	0.13
	ENT	-0.10	0.06	14196.61	-1.65	0.10
O1	(Intercept)	3.34	0.35	27.45	9.50	0.00
	RLU	0.29	0.13	2928.73	2.28	0.02
	CON	0.05	0.07	1488.48	0.71	0.48
	SKE	0.13	0.13	7837.67	1.01	0.31
	KUR	0.18	0.08	13846.89	2.24	0.02
	ENT	-0.12	0.07	15063.52	-1.62	0.10
O2	(Intercept)	3.69	0.33	28.66	11.28	0.00
	RLU	0.16	0.13	3619.07	1.29	0.20
	CON	0.03	0.07	1911.15	0.45	0.66
	SKE	0.04	0.13	9329.79	0.28	0.78
	KUR	0.13	0.08	14975.95	1.59	0.11
	ENT	-0.18	0.07	15932.07	-2.40	0.02
Oz	(Intercept)	4.11	0.37	28.25	10.97	0.00
	RLU	0.23	0.13	3482.22	1.69	0.09
	CON	-0.03	0.08	1825.14	-0.45	0.66
	SKE	0.06	0.13	9046.57	0.41	0.68
	KUR	0.14	0.08	14776.83	1.64	0.10
	ENT	-0.15	0.08	15779.51	-1.94	0.05
PO7	(Intercept)	1.85	0.26	27.39	7.23	0.00
	RLU	0.26	0.11	2328.74	2.27	0.02
	CON	0.15	0.06	1138.59	2.36	0.02
	SKE	0.17	0.11	6326.12	1.52	0.13
	KUR	0.21	0.07	12439.76	2.85	0.00
	ENT	-0.10	0.07	13960.73	-1.51	0.13
PO8	(Intercept)	2.22	0.30	27.46	7.41	0.00
	RLU	0.10	0.11	2899.51	0.93	0.35
	CON	0.14	0.06	1473.34	2.22	0.03
	SKE	-0.01	0.11	7798.35	-0.05	0.96
	KUR	0.10	0.07	13819.59	1.39	0.16
	ENT	-0.16	0.07	15039.37	-2.42	0.02

B Oculomotor model coefficients

		Estimate	Std. Error	df	t value	Pr(>|t|)
CP2	(Intercept)	0.12	0.28	26.19	0.41	0.68
	FDU	-0.06	0.07	18517.25	-0.92	0.36
	SDC	-0.15	0.07	18819.59	-2.33	0.02
	PSA	0.48	0.07	18763.95	7.26	0.00
	SSA	-0.08	0.06	18817.26	-1.19	0.24
Fpz	(Intercept)	1.80	0.29	27.33	6.24	0.00
	FDU	-0.15	0.06	18659.30	-2.79	0.01
	SDC	-0.25	0.06	18812.29	-4.55	0.00
	PSA	0.29	0.06	18802.10	5.20	0.00
	SSA	-0.01	0.05	18814.34	-0.23	0.82
P1	(Intercept)	1.36	0.35	27.65	3.90	0.00
	FDU	-0.11	0.07	18621.36	-1.70	0.09
	SDC	-0.21	0.07	18814.15	-3.08	0.00
	PSA	0.52	0.07	18791.77	7.83	0.00
	SSA	-0.05	0.07	18815.35	-0.80	0.43
P2	(Intercept)	1.54	0.40	27.65	3.85	0.00
	FDU	-0.12	0.07	18694.37	-1.84	0.07
	SDC	-0.22	0.07	18808.13	-3.35	0.00
	PSA	0.56	0.07	18808.48	8.47	0.00
	SSA	-0.05	0.07	18811.74	-0.79	0.43
P4	(Intercept)	1.42	0.40	27.37	3.57	0.00
	FDU	-0.10	0.06	18687.05	-1.66	0.10
	SDC	-0.13	0.06	18807.62	-2.07	0.04
	PSA	0.42	0.06	18805.41	6.77	0.00
	SSA	-0.05	0.06	18811.30	-0.79	0.43
Pz	(Intercept)	1.43	0.38	27.78	3.74	0.00
	FDU	-0.13	0.07	18673.66	-1.81	0.07
	SDC	-0.25	0.07	18810.75	-3.54	0.00
	PSA	0.60	0.07	18804.89	8.70	0.00
	SSA	-0.06	0.07	18813.53	-0.84	0.40